# Evidence Supporting LI-RADS Major Features for CT- and MR Imaging–based Diagnosis of Hepatocellular Carcinoma: A Systematic Review[1]

An Tang, MD, MSc
Mustafa R. Bashir, MD
Michael T. Corwin, MD
Irene Cruite, MD
Christoph F. Dietrich, MD, PhD, MBA
Richard K. G. Do, MD, PhD
Eric C. Ehman, MD
Kathryn J. Fowler, MD
Hero K. Hussain, MD
Reena C. Jha, MD
Adib R. Karam, MD[2]
Adrija Mamidipalli, MD
Robert M. Marks, MD
Donald G. Mitchell, MD
Tara A. Morgan, MD
Michael A. Ohliger, MD, PhD
Amol Shah, MD
Kim-Nhien Vu, MD
Claude B. Sirlin, MD
For the LI-RADS Evidence Working Group

The Liver Imaging Reporting and Data System (LI-RADS) standardizes the interpretation, reporting, and data collection for imaging examinations in patients at risk for hepatocellular carcinoma (HCC). It assigns category codes reflecting relative probability of HCC to imaging-detected liver observations based on major and ancillary imaging features. LI-RADS also includes imaging features suggesting malignancy other than HCC. Supported and endorsed by the American College of Radiology (ACR), the system has been developed by a committee of radiologists, hepatologists, pathologists, surgeons, lexicon experts, and ACR staff, with input from the American Association for the Study of Liver Diseases and the Organ Procurement Transplantation Network/United Network for Organ Sharing. Development of LI-RADS has been based on literature review, expert opinion, rounds of testing and iteration, and feedback from users. This article summarizes and assesses the quality of evidence supporting each LI-RADS major feature for diagnosis of HCC, as well as of the LI-RADS imaging features suggesting malignancy other than HCC. Based on the evidence, recommendations are provided for or against their continued inclusion in LI-RADS.



*Online supplemental material is available for this article.*

[1] From the Department of Radiology, Université de Montréal, 1000 rue Saint-Denis, Montréal, QC, Canada H2X 0C2 (A.T., K.N.V.); the complete list of author affiliations is listed at the end of this article. Received April 18, 2017; revision requested May 25; revision received July 4; accepted July 19; final version accepted August 15. **Address correspondence to** A.T. (e-mail: *an.tang@umontreal.ca*).

A.T. supported by a research scholarship from Fonds de Recherche du Québec-Santé and Fondation de l'Association des Radiologistes du Québec (FRQS-ARQ 26993).

**Current address:**
[2] Department of Radiology, Brown University School of Medicine, Providence, RI.

Imaging plays a critical role in the management of hepatocellular carcinoma (HCC) in at-risk patients. In contrast to other cancers, imaging is frequently used to establish the diagnosis of HCC noninvasively (1,2). Further, if a definitive diagnosis can be established by means of imaging, clinical practice guidelines do not mandate pathologic confirmation prior to treatment (3–9).

Since 2001, numerous international scientific organizations and societies have proposed imaging-based systems for the diagnosis of HCC (10). Over time, these diagnostic systems have grown in sophistication and rigor, incorporating combinations of imaging features on various modalities into diagnostic algorithms. Despite their advancement over the years, these imaging-based diagnostic systems have some persistent limitations and inconsistencies.

In 2008, the American College of Radiology convened a committee to develop a standardized Liver Imaging Reporting and Data System (LI-RADS) for interpretation, reporting, and data collection of imaging studies in patients at risk for developing HCC (1). The committee was composed mainly of diagnostic radiologists, but also hepatologists, surgeons, pathologists, and interventional radiologists. In addition to establishing a standardized lexicon and comprehensive imaging algorithm with high specificity for HCC, the committee was motivated to maintain congruence with the HCC diagnostic imaging components of the American Association for the Study of Liver Diseases (AASLD) and the Organ Procurement and Transplantation Network/United Network for Organ Sharing (OPTN/UNOS) systems (4,11,12).

In this narrative review, we summarize and assess the quality of evidence supporting each LI-RADS major feature for diagnosis of HCC, as well as of the LI-RADS imaging features suggesting malignancy other than HCC. Based on the evidence, we provide recommendations for or against their continued inclusion in the LI-RADS version 2017 update. Since the focus is on major features, this review does not address the evidence related to ancillary features, including transitional phase or hepatobiliary phase hypointensity, which can only be seen with the use of hepatobiliary contrast agents.

## Essentials

- Arterial phase hyperenhancement (APHE) is a sensitive imaging feature for progressed hepatocellular carcinoma (HCC) in at-risk patients and, in combination with "washout," provides high specificity.
- Larger observation diameter is a predictor of malignancy and facilitates noninvasive imaging diagnosis of HCC in at-risk patients.
- Washout appearance, in combination with APHE, provides high positive predictive value for HCC in at-risk patients.
- Based on limited evidence, capsule appearance provides high specificity for HCC at-risk patients.
- Although prospectively validated estimates of diagnostic accuracy are lacking, indirect evidence and biologic plausibility indicate that growth is a feature of malignancy and helps to differentiate HCC from benign entities.

## Methods

This systematic review was developed by the LI-RADS Evidence Working Group. The study protocol was not registered. The topics for the review were chosen by members of the Working Group based on priorities identified by internal survey. The Working Group was divided into six subgroups, each comprising three or four members and each assigned to a different topic—either one of the five LI-RADS major features (arterial phase hyperenhancement [APHE], observation diameter, washout appearance, capsule appearance, threshold growth) or to the LI-RADS feature set suggesting non-HCC malignancy. While the selection of five major features was based on expert opinion, the literature review was performed to ensure that imaging-based diagnostic criteria were able to achieve near-100% specificity for the noninvasive diagnosis of HCC. This review focused on the evidence supporting the inclusion of imaging features and did not attempt to gather evidence on the composition of the LI-RADS diagnostic algorithm and probability of HCC for different combinations of criteria (other than the hallmark combination of APHE and washout appearance) in the LI-RADS diagnostic table.

Each subgroup was charged with developing key research questions and then critically reviewing the literature to answer research questions thematically related to its assigned topic.

### Search Strategy

The PICO (patient population, intervention, comparison, and outcome) format frequently used in structured reviews does not lend itself well to studies of diagnostic performance. Rather than using PICO-style questions to guide the searches, therefore, the subgroups formulated free-form questions in advance with feedback from the other subgroups. A total of 10 questions were formulated under the framework and with the understanding that their answers would inform recommendations for removing or continuing to include the corresponding LI-RADS features. After the questions were formulated, each subgroup searched the PubMed

https://doi.org/10.1148/radiol.2017170554

Content codes: GI OI

**Radiology 2018;** 286:29–48

**Abbreviations:**
AASLD = American Association for the Study of Liver Diseases
APHE = arterial phase hyperenhancement
HCC = hepatocellular carcinoma
ICC = intrahepatic cholangiocarcinoma
LI-RADS = Liver Imaging Reporting and Data System
OPTN/UNOS = Organ Procurement and Transplantation Network/United Network for Organ Sharing
TVDT = tumor volume doubling time

Conflicts of interest are listed at the end of this article.

database using the search queries listed in Appendix E1 (online) and without publication date restrictions. Restrictions were applied to only include studies pertaining to humans and published in English.

### Inclusion Criteria and Data Extraction

Publications resulting from the searches were assessed by members of each working subgroup. Inclusion was based on title or abstract. Disagreements in the inclusion process were resolved by consensus discussion within each working group. For each LI-RADS major imaging features and imaging features suggesting malignancy other than HCC, the authors reviewed the full-text articles to summarize *(a)* the biologic basis and rationale, *(b)* evidence supporting or refuting their continued inclusion, *(c)* estimates of diagnostic performance or tumor volume doubling time, and *(d)* knowledge gaps.

Three challenges were encountered by every subgroup in its literature review. One challenge was that source manuscripts used inconsistent terminology. To address terminology differences and achieve internal consistency, the subgroup members in consensus converted the source terms to their closest LI-RADS equivalents. Another challenge was that source manuscripts used different reference standards. Accordingly, each subgroup was instructed to accept composite reference standards—that is, including a combination of follow-up imaging and pathology, even if the details varied across studies. A third challenge was that most studies reported the performance of features in a limited number of combinations. The combinations were not consistent across studies, it was not possible to extract the performance of individual features, and not all possible feature combinations were analyzed. For many manuscripts, moreover, the rationale for selecting particular feature combinations was not provided, including whether the combinations were selected a priori or only after data analysis.

### Quality Assessment

Based on its review, each subgroup summarized and assessed the quality of the evidence supporting inclusion of its assigned feature or feature set. Recommendations then were issued according to the Grades of Recommendation Assessment, Development, and Evaluation (GRADE) system, as this is used by the AASLD for developing its newest clinical practice guidelines (13,14). Members of the LI-RADS Evidence Working Group voted independently and were blinded to each other's votes via SurveyMonkey on the quality of evidence and strength of recommendations reported below. The options that gathered the most votes were selected. The GRADE benchmarks and survey results are reported in Appendix E2 (online).

## LI-RADS Major Imaging Criteria

### 1. Arterial Phase Hyperenhancement

*Literature review question.*—Should APHE be included as a major imaging criterion for the diagnosis of HCC?

*Definition.*—In LI-RADS, APHE refers to the presence of non-rimlike enhancement in all or part of an observation in the arterial phase that is unequivocally greater than that of the liver. To qualify, the enhancing portion must have higher intensity (magnetic resonance [MR] imaging) or attenuation (computed tomography [CT]) than background liver in the arterial phase (Fig 1). APHE (not rim) must be distinguished from rim APHE, which is a spatially defined subtype of APHE in which arterial phase enhancement is most pronounced in observation periphery. Unlike APHE, which is a major feature of HCC (discussed in this section), rim APHE suggests malignancy other than HCC (discussed in the section on imaging features suggesting malignancy other than HCC).

*Biologic basis and rationale.*—The biologic basis of APHE as a major feature of HCC is that during hepatocarcinogenesis the intranodular blood supply undergoes characteristic changes that eventually culminate in elevated arterial flow (15,16). Initially, precursor nodules such as dysplastic nodules and early HCCs have similar or even lower arterial flow than background liver. As nodules advance to progressed (overtly malignant) HCC, they develop high arterial flow due to angiogenesis and formation of nontriadal or unpaired neoarteries (15). The formation of neoarteries and the accompanying high arterial flow manifests as APHE at dynamic imaging.

*Evidence.*—The search query identified 342 studies. After reviewing the abstracts, 18 studies were considered relevant and the full text of each was reviewed. Among the included studies, 14 were retrospective and four were prospective.

Six studies reported that APHE is more sensitive than other dynamic contrast enhancement features (eg, washout appearance, capsule appearance) for diagnosis of progressed (ie, malignant neoplasm with ability to invade vessels and metastasize) HCC, with reported sensitivities ranging from 65% to 96% (17–22). Because of its high reported sensitivity for progressed HCC, APHE has been included in virtually all imaging algorithms for HCC. The majority of diagnostic studies listed in Table 1 were retrospective, however, and are prone to incorporation and verification bias. As a result, the performance reported in the radiology literature for APHE for detecting progressed HCC may be overestimated. Supporting this supposition, studies using explant pathology have reported a lower overall sensitivity of 74%, ranging from 43% to 53% for lesions smaller than 1 cm (23,24). Studies validated by means of explant pathology may reflect more closely the sensitivity for detecting HCC as they are less confounded by verification bias, although selection bias remains a potential problem. Overcoming selection bias is a persistent challenge for radiology research, as it is neither ethical nor feasible to biopsy all nodules or to explant every liver.

Compared with its sensitivity for progressed HCC, APHE has low sensitivity for early, very well differentiated HCCs due to incomplete neovascularization and for poorly differentiated HCCs due to conversion to glycolytic metabolism and shut down of angiogenesis, but the exact sensitivities in these lesions is unclear (25).

**Figure 1**

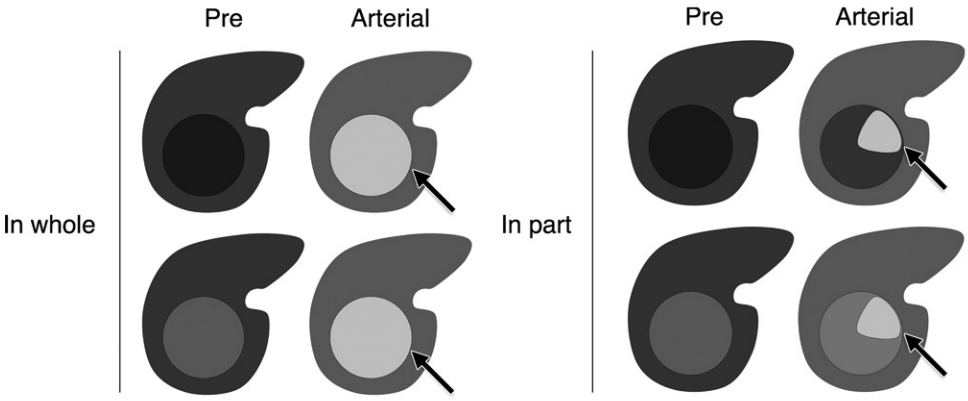


a.

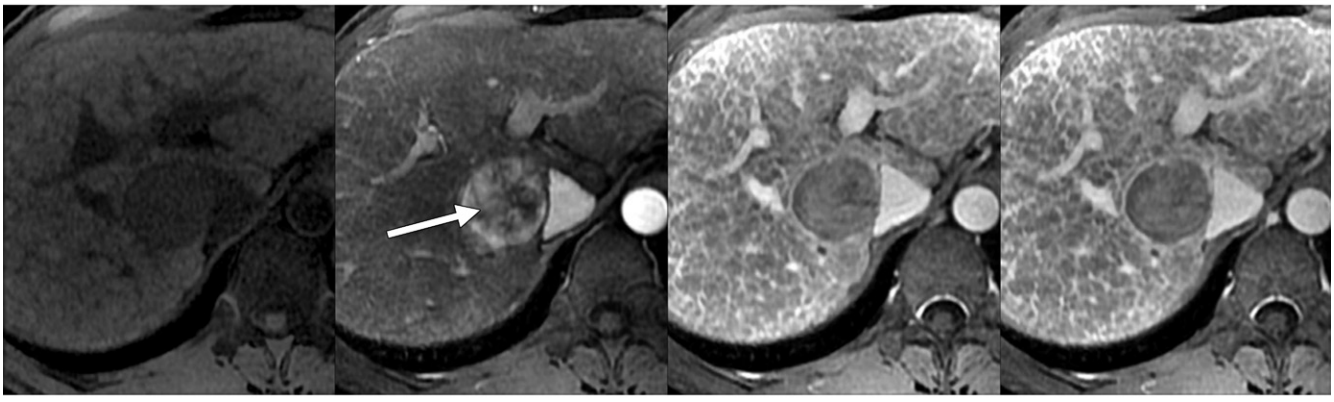

b.

**Figure 1:** **(a)** Schematic of APHE (arrows). **(b)** Images in a 53-year-old man with HCC and hepatitis C virus cirrhosis. T1-weighted three-dimensional gradient-recalled echo images with fat suppression obtained in (from left to right) unenhanced, late arterial, portal venous, and 3-minute delayed phases after administration of gadolinium-based contrast agent show APHE (arrow) in the late arterial phase. LI-RADS schematic reproduced with permission from the American College of Radiology.

**Table 1**

**Diagnostic Performance of APHE**

| Study and Reference No. | No. of Patients / No. of Nodules | Modality | Unit of Analysis | AUC | Sensitivity (%) | Specificity (%) | PPV (%) | NPV (%) |
|---|---|---|---|---|---|---|---|---|
| Oliver et al (19) | 42/157 | CT | Per nodule | ... | 76 | ... | ... | ... |
| Yamashita et al (20) | 42/72 | CT | Per nodule | 0.87 | ... | ... | ... | ... |
| | | MR imaging | Per nodule | 0.96 | ... | ... | ... | ... |
| Laghi et al (131) | 77/140 | CT | Per nodule | ... | 87 | ... | 94 | ... |
| Lee et al (18) | 51/51 | CT | Per patient | ... | 96 | ... | ... | ... |
| Forner et al (29) | 89/89 | MR imaging | Per patient | ... | 85 | 90 | 94 | 74 |
| Pitton et al (132) | 28/162 | CT | Per nodule | ... | 74 | ... | ... | ... |
| | | MR imaging | Per nodule | ... | 98 | ... | ... | ... |
| Sangiovanni et al (21) | 64/67 | CT | Per nodule | ... | 65 | 81 | 85 | 59 |
| | | MR imaging | Per nodule | ... | 66 | 62 | 72 | 54 |
| Kim et al (17) | 96/116 | MR imaging | Per nodule | ... | 84 | 75 | 67 | 89 |
| Rimola et al (22) | 159/159 | MR imaging | Per patient | ... | 85 | 64 | 81 | 71 |
| An et al (38) | 86/135 | MR imaging | Per nodule | ... | 76 | 97 | 99 | 55 |

Note.—AUC = area under the receiver operating characteristic curve, PPV = positive predictive value, NPV = negative predictive value.

**Figure 2**

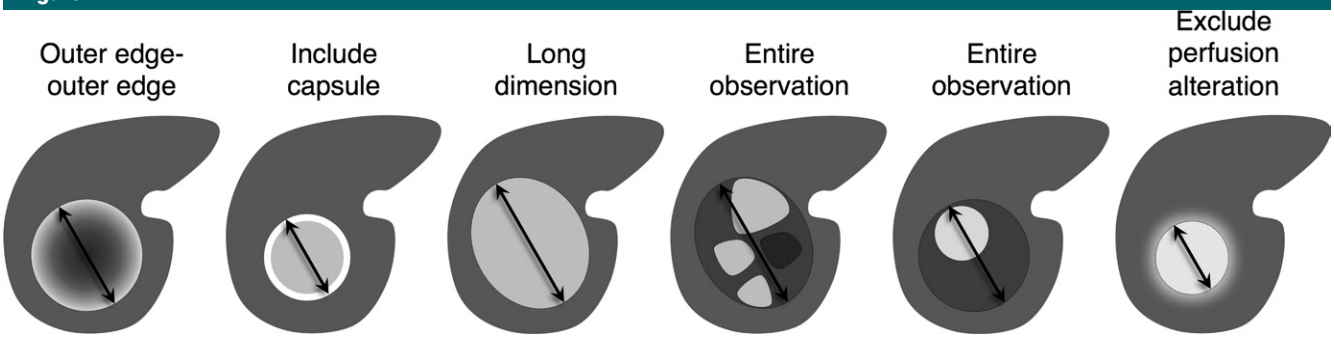


**Figure 2:** Schematic of observation diameter indicating measurement conventions recommended in LI-RADS (arrows). LI-RADS schematic reproduced with permission from the American College of Radiology.

Another limitation is that APHE lacks specificity for HCC, as this feature can be present in benign entities such as hemangiomas and perfusion anomalies, premalignant lesions such as dysplastic nodules, and non-HCC malignant lesions such as intrahepatic cholangiocarcinomas (ICCs) (although rim APHE is observed with ICCs). For these reasons, the positive predictive value of APHE is not sufficient for it to be a sole diagnostic imaging criterion for HCC. In studies that have included lesions other than HCC, the positive predictive value of APHE ranges 65%–81% (22,26–28), indicating that a meaningful number of observations with APHE are not HCC.

Combining APHE and "washout" increases specificity for the diagnosis of HCC (26). Many studies have shown high specificities and positive predictive value, varying from 81% to 100% and from 87% to 100%, respectively, with acceptable sensitivities, varying from 43% to 98%, when liver nodules demonstrated both APHE and washout (21,22,29–31). However, this increase in specificity is associated with a reduction in sensitivity, especially in smaller-sized lesions, where washout is less pronounced and APHE may be the only major feature present (22,29,30,32).

*Knowledge gaps.*—APHE has been included in virtually all imaging algorithms for HCC (4,11,33–37). Nevertheless, further research is necessary to evaluate diagnostic performance of APHE according to cirrhosis severity, imaging modality, and type of contrast agent. According to LI-RADS, APHE may be in whole or in part; the performance of APHE in whole and APHE in part should be investigated independently. The sensitivity and positive predictive value of APHE should be assessed in studies controlling verification and incorporation bias. Prospective studies are needed with inclusion of a suitably large number of representative benign and malignant non-HCC lesions in addition to HCCs spanning the carcinogenesis spectrum. The sensitivity of APHE for early HCC or for some highly aggressive infiltrative HCCs should be clarified. Future research is needed to determine if the diagnosis of HCC in these cases can be established reliably in the absence of APHE. APHE can be missed due to arterial phase mistiming. Research is needed to assess whether emerging high-temporal-resolution MR imaging techniques that improve arterial phase capture increase the sensitivity of APHE for detecting HCC. In the majority of studies, APHE has been assessed on the native contrast-enhanced images rather than subtraction images (38); thus, the incremental value of subtractions is not well understood.

*Summary.*—APHE is a sensitive imaging feature for progressed HCC in at-risk patients and, in combination with "washout," provides high specificity.

**Recommendation:**

1. APHE should be a major criterion for the diagnosis of HCC.

Quality of evidence: Moderate.

Strength of recommendation: Strong.

### 2. Observation Diameter

*Literature review questions.*—*(a)* Should observation diameter be included as a major imaging feature for the diagnosis of HCC? *(b)* What particular sequence or phase for diameter should be used for measurement?

*Definition.*—In LI-RADS, diameter is defined as the largest dimension from outer edge to outer edge of an observation (Fig 2). LI-RADS currently uses two diameter thresholds to stratify the risk of HCC: 10 and 20 mm.

While many publications have classified observations by size qualitatively (eg, "small" HCC), the qualitative meanings have evolved in parallel with improvements in imaging technology. HCCs were considered "small" if smaller than 50 mm in the 1980s (39,40), smaller than 30 mm in the following 2 decades (41–45), and smaller than 20 mm in the most recent publications (29,46,47). It is therefore preferable to report observation diameter quantitatively by using a continuous measure or a precisely defined diameter interval rather than use qualitative terms.

*Biologic basis and rationale.*—It is now well established that in multistep hepatocarcinogenesis, progressively more aggressive clonal cell populations acquire a survival advantage, gradually replace the neighboring cells, and expand to form successively less-differentiated nodules. As shown in numerous pathology studies conducted mainly in the 1980s and 1990s, premalignant nodules rarely grow larger than about 15 mm (48–51). As nodules progress to overt malignancy,

cellular proliferation increases and the nodules may grow to larger sizes. Thus, nonmalignant regenerative and dysplastic nodules typically are smaller than 15 mm and rarely exceed 20 mm. By comparison, HCCs may span a wide spectrum of size from tiny to massive.

*Evidence.*—The search query identified 247 studies for question 2a. After reviewing the abstracts, 31 were considered relevant and the full text of each was reviewed. Among the included studies, 26 were retrospective and five were prospective.

All included imaging studies showed an association between nodule diameter and HCC likelihood in at-risk patients. The relationship between diameter and HCC likelihood was observed regardless of the applied stratification threshold (nodules ≤ 10 mm versus 11–20 mm [49], < 10 mm versus 10–15 mm versus 16–20 mm [29], < 13 mm versus ≥ 13 mm [52], and 10–20 mm versus 20–30 mm [53]) and regardless of the reference standard (histopathologic evaluation alone [49], changes at follow-up imaging [52], or composite [29,53]).

In addition to its biologic basis, size contributes to the diagnosis of HCC due to a technical consideration: larger observations are easier to detect and characterize with imaging techniques, thus reducing both false-negative and false-positive results. Several studies have shown higher sensitivity with larger observation diameters for different size stratification thresholds: (< 10 mm versus 11–20 mm [49], < 10 mm versus 10–20 mm versus ≥ 20 mm [54,55], < 20 mm versus ≥ 20 mm [56–59]). This has been shown in the setting of single-center studies (49,54,56,57) and in meta-analyses (55,58,59) of diagnostic test accuracy. Similarly, studies have reported either an increase in specificity (60) or similar specificity (57,61) with larger observation size. A meta-analysis by Chou et al has found increases in pooled specificity from 86% to 90% with CT and from 95% to 98% with MR imaging for observations 10–20 mm versus greater than 20 mm (62). In 102 patients undergoing liver transplantation based on clinical and radiologic findings, pathologic examination of the explanted livers showed lower false-positive rates with increasingly larger size stratification thresholds: 10 mm or less versus 20 mm or less versus 30 mm or less versus greater than 30 mm (60). Since both sensitivity and specificity tend to be higher for larger lesions, overall diagnostic accuracy tends to be better (58,63). Higher areas under the receiver operating characteristic curves have been achieved for diagnosis of HCCs of all size than for tumors 15 mm or smaller (63).

Six articles relevant to question 2b were identified (64–69). No article assessed the accuracy of imaging phase or sequence for measuring diameter, since there is no valid method for establishing the reference value in vivo. Instead, studies have examined interreader agreement on assessment of observation diameter (64–68). These studies report near-perfect agreement on observation diameter, with intraclass correlation coefficients between 0.94 and 0.98 for repeatability of observation diameter between dynamic imaging phases (66) and κ of 0.99 for agreement on the vascular phase that best demonstrated the observation (65,67). However, these studies relied on an observation atlas depicting individual observations (66) or on the single series that provided the best visualization (65,67). Among those studies, only one analyzed the effect of vascular phase on reader agreement: Davenport et al (66) found that the agreement was consistent across all vascular phases in which an observation was visible and that no vascular phase provided significantly higher agreement. No study has assessed the effect of imaging sequence on diameter agreement.

*Knowledge gaps.*—Despite the importance of nodule diameter, most publications in the radiology literature, even those that have assessed the diagnostic value of diameter, have not described how nodules were measured, leaving the definition of this critical feature ambiguous. To address this ambiguity, LI-RADS has provided a precise definition of diameter and advocates measuring observation diameter on the sequence, phase, and imaging plane in which the margins are most sharply demarcated and in which there is no anatomic distortion. Since the apparent diameter in the arterial phase may be affected by the exact timing of image acquisition and perilesional enhancement, LI-RADS recommends diameter measurement in nonarterial phases whenever possible, even though this does not affect reader agreement as shown by Davenport et al (66). By comparison, the OPTN/UNOS guidelines require that diameter be measured in the arterial phase, despite the potential for timing-related variability. Scientific evidence is lacking for recommending a particular sequence, phase, and imaging plane for measuring observation diameter. Further research is needed to systematically assess sources of variability—including imaging modality, imaging phase, imaging technique, type of contrast agent, and reader—in measuring observation diameter without prior selection of image on which measurement should be performed. Research is also needed to assess the impact on observation diameter measurement of multiarterial phase acquisitions by using emerging high-temporal-resolution techniques (70,71). These knowledge gaps also apply to threshold growth as discussed below.

In 2005, the AASLD selected thresholds of 10 and 20 mm, and these were subsequently adopted by other organizations (10). Further research is needed to determine if these thresholds should be modified. As technology advances, the ability to characterize smaller nodules improves. Hence, it is plausible that smaller thresholds may maintain similar specificity while improving sensitivity.

*Summary.*—Larger observation diameter is a predictor of malignancy and facilitates noninvasive imaging diagnosis of HCC in at-risk patients.

**Recommendation:**

2a. Observation diameter thresholds of 10 mm and 20 mm should be a major criterion for the diagnosis of HCC.

Quality of evidence: Moderate.

Strength of recommendation: Strong.

2b. Observation diameter should be measured on the sequence or phase in which the margins are most sharply demarcated and in which there is no anatomic distortion.

**Figure 3**

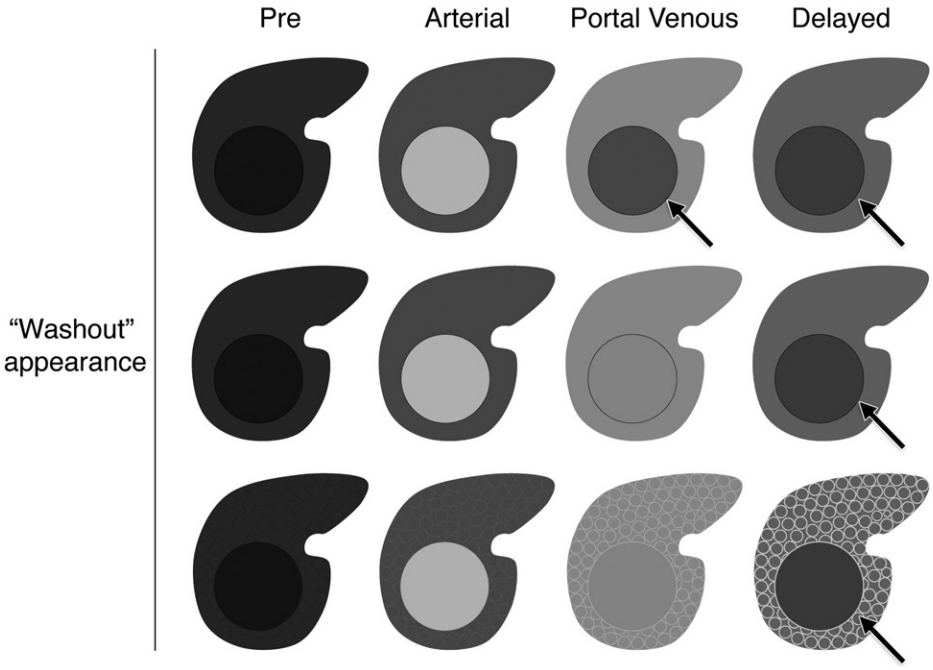


**Figure 3:** **(a)** Schematic of APHE (all rows) and washout appearance (arrows) of entire observation in portal venous and delayed phase (top row), washout in delayed phase (middle row), and washout in delayed phase relative to liver parenchyma which consists of nodules and fibrosis (bottom row). **(b)** Images in a 57-year-old man with HCC and hepatitis C virus cirrhosis. Axial CT images obtained in (from left to right) unenhanced, late arterial, portal venous, and 3-minute delayed phases after administration of an iodinated contrast agent show washout appearance most conspicuous in the 3-minute delayed phase (arrow). LI-RADS schematic reproduced with permission from the American College of Radiology.

a.

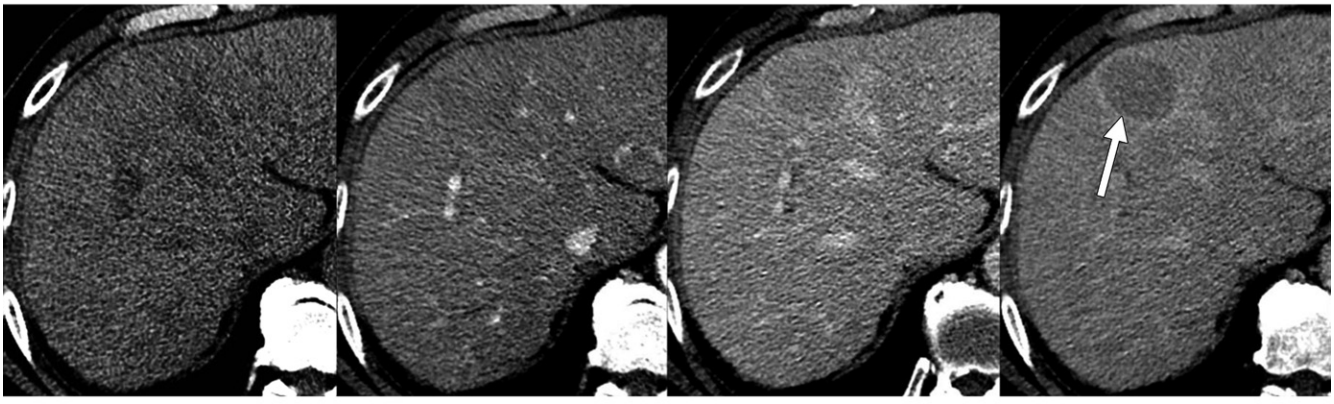

b.

Quality of evidence: Low.

Strength of recommendation: Weak.

2c. Observation diameter should not be measured in the arterial phase if the margins are clearly visualized on another phase or sequence.

Quality of evidence: Low.

Strength of recommendation: Weak.

### 3. Washout Appearance

*Literature review question.*—Should "washout" be included as a major imaging criterion for the diagnosis of HCC?

*Definition.*—In LI-RADS, washout appearance or "washout" is defined as a dual concept that includes *(a)* visually assessed temporal reduction in enhancement relative to liver from an earlier to a later phase resulting in *(b)* extracellular phase hypoenhancement relative to the background liver (Fig 3). The extracellular phase is the phase in which liver enhancement is attributable mainly to extracellular distribution of a contrast agent. Operationally, this refers to the portal venous phase and the 3- to 5-minute delay if an extracellular agent or gadobenate is given and to the portal venous phase only if gadoxetate is given. Thus, hypointensity in the transitional phase (which occurs about 2–5 minutes after injection of gadoxetate disodium and corresponds temporally to the delayed phase after injecting extracellular space agents) does not qualify as "washout." If the liver parenchyma visually consists of both nodules and fibrosis, then enhancement of the observation should be compared with that of the composite liver tissue (ie, a visual average of the nodules and fibrosis). If

**Table 2**

**Diagnostic Performance of Washout Appearance as a Standalone Feature**

| Study and Reference No. | No. of Patients/No. of Nodules | Modality | Unit of Analysis | AUC | Sensitivity (%) | Specificity (%) | PPV (%) | NPV (%) |
|---|---|---|---|---|---|---|---|---|
| Sangiovanni et al (21) | 64/67 | CT | Per nodule | ... | 53 | 100 | 100 | 57 |
| | | MR imaging | Per nodule | ... | 59 | 95 | 95 | 61 |
| Kim et al (17) | 96/116 | MR imaging | Per nodule | ... | 79 | 62 | 55 | 83 |
| Rimola et al (22) | 159/159 | MR imaging in portal venous phase | Per patient | ... | 50 | 89 | 90 | 49 |
| | | MR imaging in delayed phase | Per patient | ... | 68 | 88 | 91 | 60 |

Note.—AUC = area under the receiver operating characteristic curve, PPV = positive predictive value, NPV = negative predictive value.

only a portion of the observation shows APHE, the component with washout does not need to correspond to the component that demonstrates APHE, however the component does need to enhance from earlier to later phase for this feature to be present. LI-RADS advocates the terms washout appearance or "washout" (with quotes) over washout (without quotes), because—as discussed below—washout appearance relies on subjective perception which may be an optical illusion, rather than representing true washout.

*Biologic basis and rationale.*—"Washout" is considered a strong predictor and major criterion of HCC for most imaging algorithms (4,10–12,36). The visual perception of washout can result from true de-enhancement of a nodule, greater enhancement of the surrounding liver, or a combination of both factors. These in turn have been attributed to diminished portal venous blood supply, high tumoral cellularity with associated small extracellular volume (15,16,72), and expanded extracellular space of the surrounding fibrotic liver. Additionally, the concomitant presence of capsule appearance may produce an optical illusion of "washout" not confirmed by objective measurement of signal intensity (68). Finally, intrinsic hypoattenuation or hypointensity before contrast agent injection may contribute to the perception of "washout." Based on current knowledge, washout appearance should be considered absent if its perception is due entirely to optical illusion from the enhancing capsule (68). On the other hand, washout appearance should be considered present even if intrinsic hypoattenuation or hypointensity is contributory.

*Evidence.*—The search query identified 135 studies. After reviewing the abstracts, 25 studies were considered relevant and the full text of each reviewed. Among the included studies, 18 were retrospective and seven were prospective.

Included studies reported the diagnostic performance of "washout" by using histopathologic evaluation alone or a combination of histopathologic evaluation and follow-up imaging, as reference standards. These studies did not attempt to distinguish the factors underlying the perception of "washout" (eg, nodule de-enhancement, parenchymal hyperenhancement, optical illusion), Most studies were single center, had limited sample sizes (64–159 patients, 50–159 individual lesions), and assessed the combination of "washout" and APHE, rather than "washout" alone, as a criterion for HCC. Table 2 summarizes the diagnostic performance of washout appearance alone and Table 3 the combination of APHE and "washout." Two prospective studies compared the diagnostic performance of "washout" alone with that of combined "washout" and APHE and found "washout" alone to have lower specificity and positive predictive value (21,22).

Using extracellular agents, "washout" may be perceived during the portal venous phase or delayed venous phases. However, three included studies showed greater perceptibility of this feature in the delayed phase (22,30,73). Luca et al reported a 59% increase in HCC detection by using the delayed phase compared with the portal venous phase (30). These results support the inclusion of delayed phase imaging in multiphasic protocols for HCC.

With one exception, all included studies defined "washout" subjectively. A prospective study by Liu et al evaluated an objective method of quantifying "washout" at multiphasic CT. These authors reported that a percentage attenuation ratio of 107 or greater yielded a sensitivity, specificity, and positive and negative predictive values of 100%, 75.8%, 63.6%, and 100%, respectively, for characterization of washout, with histopathologic findings on explanted livers used as the reference standard (74). Their results revealed that while quantitative assessment of washout showed better sensitivity than qualitative assessment, this improvement is obtained at the expense of a higher number of false-positive findings (74). A recent retrospective study by Sofue et al showed that a lesion-to-liver signal intensity ratio of 0.88 at MR imaging correlated most strongly with readers' visual interpretation of washout (68).

Less is known about the characterization of washout with hepatobiliary agents. Although some studies have shown that transitional phase hypointensity is strongly predictive of HCCs (75–77), LI-RADS requires that "washout" after gadoxetate disodium injection be assessed in the portal venous phase, prior to the transitional or hepatobiliary phases. Due to rapid uptake of the agent by background hepatocytes, the liver is substantially enhanced in the transitional and hepatobiliary phases. As a result, relative hypointensity of an

**Table 3**

**Diagnostic Performance of APHE and Washout Appearance**

| Study and Reference No. | No. of Patients/No. of Nodules | Modality | Unit of Analysis | AUC | Sensitivity (%) | Specificity (%) | PPV (%) | NPV (%) |
|---|---|---|---|---|---|---|---|---|
| Lopez Hänninen et al (133) | 33/50 | CT | Per nodule | ... | 80 | ... | ... | ... |
| Burrel et al (23) | 50/127 | CT | Per patient | ... | 100 | 96 | ... | ... |
| | | MR imaging | Per patient | ... | 100 | 90 | ... | ... |
| | | CT | Per nodule | ... | 61 | 66 | 87 | 30 |
| | | MR imaging | Per nodule | 0.98 | 76 | 75 | 90 | 50 |
| Marrero et al (72) | 94/94 | MR imaging | Per patient | ... | 89 | 95 | 98 | 82 |
| Forner et al (29) | 89/89 | MR imaging | Per patient | ... | 62 | 97 | 97 | 55 |
| Denecke et al (24) | 30/76 | CT | Per nodule | ... | 78 | ... | 91 | ... |
| Luca et al (30) | 125/158 | CT | Per nodule | ... | 43 | 93 | 95 | 34 |
| Sangiovanni et al (21) | 64/67 | CT | Per nodule | ... | 44 | 100 | 100 | 52 |
| | | MR imaging | Per nodule | ... | 44 | 100 | 100 | 54 |
| Rimola et al (22) | 159/159 | MR imaging | Per patient | ... | 58 | 96 | 97 | 56 |
| Serste et al (31) | 74/92 | CT | Per nodule | ... | 74 | 81 | 87 | 65 |
| | | MR imaging | Per nodule | ... | 81 | 85 | 90 | 72 |
| | | CT and/or MR imaging | Per nodule | ... | 98 | 81 | 90 | 96 |
| | | CT and MR imaging | Per nodule | ... | 57 | 85 | 87 | 53 |
| Jang et al (26) | 96/110 | CT | Per nodule | ... | 57 | 99 | ... | ... |

Note.—AUC = area under the receiver operating characteristic curve, PPV = positive predictive value, NPV = negative predictive value.

observation in these phases may reflect rapid drainage of contrast material, lack of functional hepatocytes relative to background liver, or a combination of the two (63). For these reasons, transitional phase hypointensity is not specific for HCC, even in combination with APHE, and it can be seen with hemangiomas, non-HCC malignancies, some dysplastic nodules, siderotic nodules, and other benign entities. A recent study confirmed that transitional phase hypointensity can lead to false-positive interpretations and hence lower specificity for the diagnosis of HCC (77). Given its lack of specificity, transitional phase hypointensity does not have the same diagnostic implication as "washout" and does not constitute a major feature in LI-RADS.

*Knowledge gaps.*—"Washout" relies on the apparent relative hypoenhancement of HCC compared with progressively enhancing adjacent liver parenchyma during extracellular phase imaging. However, in patients with advanced cirrhosis, the liver parenchyma may have altered enhancement dynamics. In such cases, liver heterogeneity may obscure small areas of "washout." Also, the relative sensitivity and specificity of "washout" characterized with CT and MR imaging in the same subjects is not well known. Hence, further research is necessary to evaluate diagnostic performance of "washout" according to cirrhosis severity, imaging modality, and type of contrast agent. Additionally, the diagnostic potential of quantitative determination of true washout, via subtraction images or region of interest measurements at different time points, remains to be determined.

*Summary.*—Washout appearance, in combination with APHE, provides high positive predictive value for HCC in at-risk patients.

**Recommendation:**

3. "Washout" should be included as a major imaging criterion for the diagnosis of HCC.

Quality of evidence: Moderate.

Strength of recommendation: Strong.

### 4. Capsule Appearance

*Literature review question.*—In at-risk patients, should capsule appearance be included as a major imaging criterion for the diagnosis of HCC?

*Definition.*—Capsule appearance is defined as a smooth, uniform, sharp border around most or all of an observation, unequivocally thicker or more conspicuous than fibrotic tissue around background nodules, and detected as an enhancing rim in portal venous, delayed, or transitional phases (Fig 4). The rim of enhancement does not always represent a true tumor capsule and may instead represent a pseudocapsule, thought to result from perilesional compressed liver tissue. The distinction between true tumor capsule and pseudocapsule cannot be made definitely by imaging (78), but only at pathologic evaluation (78–82). This is why LI-RADS favors the terms "capsule" or capsule appearance. Importantly, capsule appearance is recognized as a major feature of HCC by the OPTN/UNOS guidelines (11) but not the AASLD guidelines (4).

*Biologic basis and rationale.*—Capsule formation is a characteristic histopathologic feature of progressed HCCs with expansile growth (78). By comparison, capsule formation is rare in early, very well-differentiated HCCs and in infiltrative, poorly differentiated HCCs, and it does not occur with ICC (83). The capsule appearance on images does not necessarily represent a true fibrous capsule but may comprise

**Figure 4**

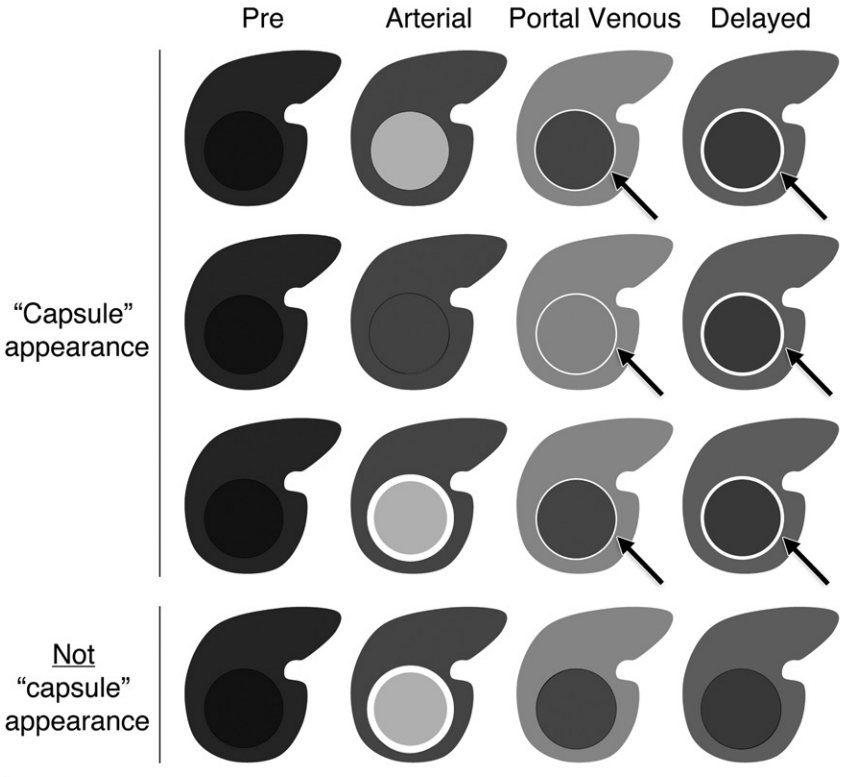


a.

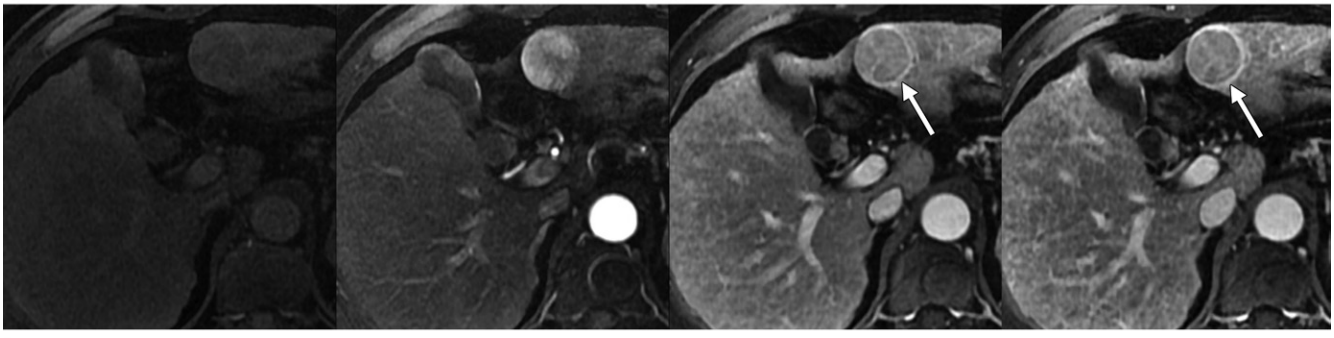

b.

**Figure 4:** **(a)** Schematic of observations with (top three rows) and without (bottom row) capsule appearance. Observations with "capsule" (arrows) show unequivocal peripheral rim enhancement in portal venous phase or delayed phase. The degree of enhancement usually is greater in the delayed phase than in the portal venous phase. Such observations may have APHE (top row and third row) or arterial phase iso- or hypoenhancement (second row). A rim of APHE also may be present. However, if rim enhancement is only seen in the arterial phase (bottom row), this should not be characterized as "capsule." **(b)** Images in a 54-year-old man with HCC and hepatitis C virus. T1-weighted 3D gradient-recalled echo images with fat suppression obtained in (from left to right) unenhanced, late arterial, portal venous, and 3-minute delayed phase after administration of gadolinium-based contrast agent show capsule appearance in portal venous and delayed phases (arrows). LI-RADS schematic reproduced with permission from the American College of Radiology.

fibrous tissue (collagen), prominent sinusoids, and/or compressed liver parenchyma at histopathologic examination (78–82). In a radiology-pathology study by Ishigami et al (78) 15 of 106 of HCCs (14.2%) had a capsule appearance at imaging that did not correlate to a true fibrous capsule at histopathologic examination. In this study, the sensitivity and specificity of MR imaging in the diagnosis of histologic fibrous capsule was 94.0% (47 of 50 "capsules" were true-positive) and 73.2% (41 of 56 "capsules" were true-negative) respectively, with an accuracy of 83.0% (88 of 106).

Histologic studies (84,85) have demonstrated that the "capsule" derives its blood supply primarily from the portal venous system, which may in part account for the delayed "capsule" enhancement on portal venous phase images. The fibrous and/or prominent sinusoidal components of the "capsule," with their expanded extracellular space, likely contribute to the characteristic progressive temporal enhancement.

*Evidence.*—The search query identified 344 studies. After reviewing the abstracts, two studies were considered relevant and the full text of each was reviewed.

Both included studies were single-center studies, one prospective and the other retrospective, and each evaluated the imaging diagnostic performance of capsule appearance (22,56) as summarized in Table 4.

**Table 4**

**Diagnostic Performance of Capsule Appearance**

| Study and Reference No. | No. of Patients/No. of Nodules | Modality | Unit of Analysis | AUC | Sensitivity (%) | Specificity (%) | PPV (%) | NPV (%) |
|---|---|---|---|---|---|---|---|---|
| Khan et al (56) | 80/116 | MR imaging | Per nodule | ... | 64 | 86 | 89 | 87 |
| Rimola et al (22) | 159/159 | MR imaging | Per patient | ... | 42 | 96 | 96 | 47 |

Note.—AUC = area under the receiver operating characteristic curve, PPV = positive predictive value, NPV = negative predictive value.

Khan et al (56) retrospectively assessed the diagnostic utility of capsule appearance as an indicator of HCC in arterially enhancing nodules 5 cm or smaller in cirrhotic liver. The study population included 80 patients with 116 nodules, 74 of which were HCC. Biopsy, explant correlation, and/or follow-up imaging were the reference standard. The sensitivity and specificity of capsule appearance for the diagnosis of HCC were, respectively, 55% and 83% for nodules smaller than 2 cm, 75% and 100% for nodules 2–5 cm, and 64% and 86% for nodules ≤ 5 cm. In general, capsule appearance had a slightly higher sensitivity but similar specificity to washout appearance. This study suggested that capsule appearance is a predictor of HCC, which, as a standalone feature or in combination with size (≥ 2 cm), may be a better predictor of HCC than washout appearance alone.

Rimola et al (22) prospectively assessed the diagnostic accuracy of capsule appearance in HCC nodules 2 cm or smaller. The study population included 159 patients in an U.S.-based surveillance program with 159 sonographically detected nodules, 103 of which were HCC measuring 9–32 mm in size. Biopsy or follow-up imaging was the reference standard. Capsule appearance had a sensitivity and specificity of 42% and 96%, respectively, which was very similar to the sensitivity and specificity of "typical vascular pattern" of HCCs of APHE with "washout" (sensitivity: 58%, specificity: 96%). This study demonstrated that capsule appearance is specific for HCC in lesions 2 cm or smaller, but its overlap with the "typical vascular pattern" of HCC limits its incremental value in overall imaging diagnostic sensitivity. In addition, capsule appearance has a relatively low frequency in observations 2 cm or smaller. As the study was restricted to sonographically detected HCCs, however, the generalizability of the results to all HCCs is unclear.

Although not identified in the formal search, three additional studies suggest that the presence of capsule appearance can help reduce the risk of mistaking small HCCs for ICCs (86–88).

*Knowledge gaps.*—Published studies have assessed capsule appearance on portal venous or delayed images and not on images obtained with other sequences. Future research is necessary to assess capsule appearance with other sequences, including T2-weighted images and the transitional and hepatobiliary phases of imaging performed with hepatobiliary agents. Further research is also needed to determine the incremental diagnostic value of "capsule" in addition to APHE and "washout," and its utility as a diagnostic criterion in observations smaller than 2 cm given its low sensitivity below this size threshold.

A recent article has shown that, in some cases, the presence of a capsule creates the visual perception of washout, even when a mass is not hypointense to background liver (68). Because this was an unrecognized phenomenon until recently, some prior studies may have failed to distinguish washout appearance from the optical illusion of washout created by an enhancing capsule. Further quantitative studies will be required to define an objective measure of "washout."

*Summary.*—Based on limited evidence, capsule appearance provides high specificity for HCC at-risk patients. Capsule appearance is a recognized feature of HCC in the OPTN/UNOS guidelines.

**Recommendation:**

4. Capsule appearance should be a major criterion for diagnosis of HCC.

Quality of evidence: Moderate.

Strength of recommendation: Strong.

### 5. Threshold Growth

*Literature review questions.*—*(a)* Should threshold growth be included as a major imaging criterion for the diagnosis of HCC? *(b)* In patients at risk for HCC, does observation growth allow differentiation of malignant from nonmalignant observations? *(c)* What is the tumor growth or doubling time for HCC, ICC, and nonmalignant tumors? *(d)* Are there imaging-based studies of diagnostic test accuracy that use growth as a reference standard for HCC or malignancy?

*Definition.*—In LI-RADS, threshold growth refers to increase in diameter of a mass compared with its baseline by a minimum of 5 mm and by at least 50% diameter increase if time interval is less than 6 months or by at least 100% diameter increase if more than 6 months. In addition, a new mass measuring at least 10 mm also represents threshold growth, regardless of the time interval (89). Definitions of threshold growth are illustrated in Figure 5. While arbitrary, the LI-RADS definition of threshold growth was dictated by the need for congruency with the OPTN/UNOS definition which requires "50% or larger in diameter increase on a CT scan or MR image obtained 6 months or less apart and that measures at least 10 mm at the time of diagnosis" (90). The "100% diameter increase if more than 6 months" was introduced by LI-RADS and based on expert opinion to address cases in

**Figure 5**

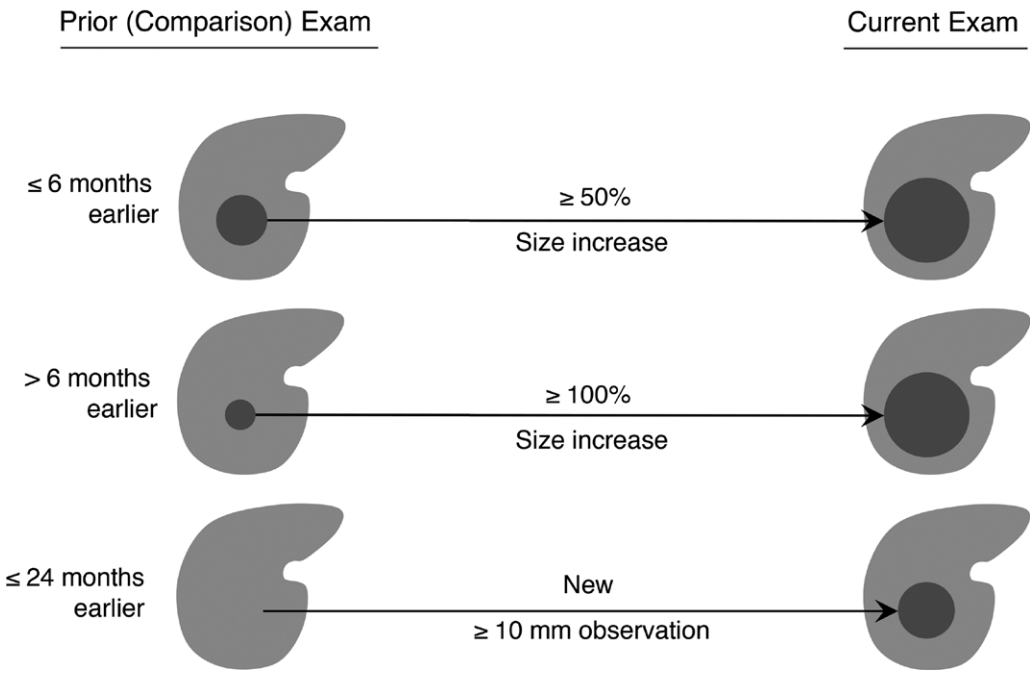


**Figure 5:** Schematic illustrates the three LI-RADS definitions of threshold growth: increase in diameter of a mass compared with its baseline by a minimum of 5 mm and by at least 50% diameter increase if time interval is less than 6 months (top row) or by at least 100% diameter increase if more than 6 months (middle row). In addition, a new mass measuring at least 10 mm that was previously unseen within the last 24 months also represents threshold growth (bottom row). LI-RADS schematic reproduced with permission from the American College of Radiology.

which the time interval between examinations exceeds 6 months (89).

*Biologic basis and rationale.*—Growth is an indicator of malignancy and, while not specific to HCC, has been studied widely in HCC (91). Measuring maximum tumor diameter on at least two serial studies assesses its doubling time. Physiologically, tumor volume doubling time (TVDT) is an indicator of the biologic potential of a tumor and its blood supply (92). While benign lesions tend to remain stable or grow slowly over time, malignant tumors grow more rapidly. Further, TVDT reflects the degree of differentiation of malignant tumors, as well-differentiated HCCs tend to grow more slowly than moderately and poorly differentiated HCCs.

*Evidence.*—The search query identified 297 studies. After reviewing the abstracts, 42 studies were considered relevant and the full text of each was reviewed. Among the included studies, 40 were retrospective and two were prospective.

Figure 6 summarizes data from retrospective studies reporting TVDT of HCCs. The natural history of HCC growth has been documented in untreated patients, who were either poor surgical candidates or have refused treatment, retrospectively when prior examinations were false-negative (86), or in treated patients with tumor recurrence. Additionally, as the growth rate of HCC varies according to its degree of differentiation and vascularization, reported TVDTs depend in part on the criteria used for tumor detection and diagnosis. Hence, the reported TVDTs may not represent those of treatment-naive HCCs eligible for curative therapy and may depend in part on study design and applied imaging technology.

Accounting for these methodological limitations, the available evidence reveals that HCCs exhibit a broad range of TVDTs, from as low as 9 days (93) to as high as several years (94,95). The median TVDT in untreated primary HCCs is 178 days, while the median TVDT of recurrent HCCs after local-regional treatment is 82 days (96).

Well-differentiated HCCs tend to be slow growing, whereas moderately and poorly differentiated HCCs are fast growing, although there is overlap in the reported TVDTs of HCCs with varying degrees of differentiation (93,97,98). Imaging features associated with shorter TVDT include APHE (92,99–101), presence of "washout" (100,102), T2 hyperintensity (99), and diameter less than 1 cm at baseline (94,103).

The TVDT of ICC in cirrhosis is unknown. In the noncirrhotic liver, it has been reported as 70 days (range, 15 to 512 days) in one study (104).

No included studies provided data on the TVDT of benign or premalignant lesions in the cirrhotic liver. The TVDT of hemangiomas in the noncirrhotic

**Figure 6**

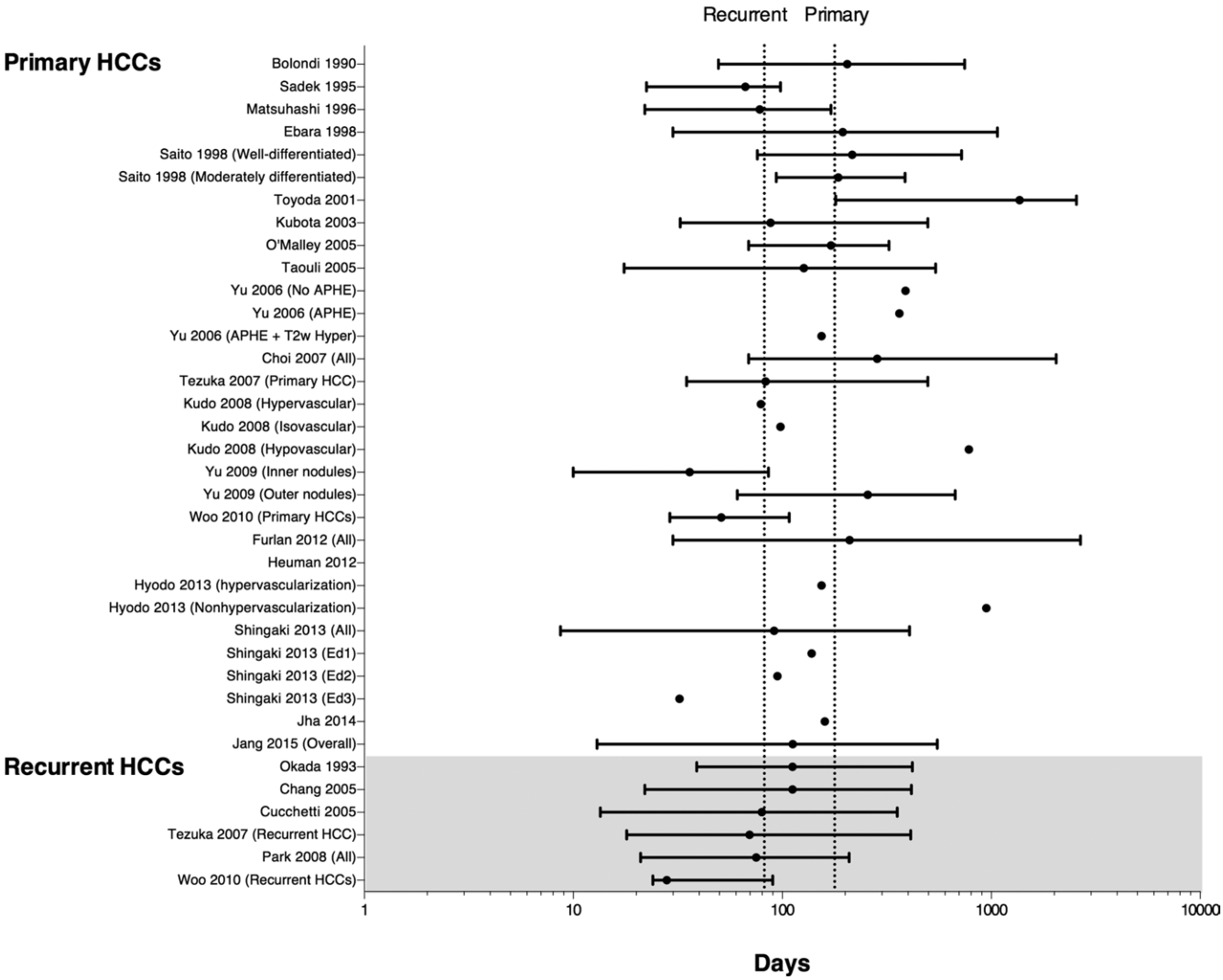


**Figure 6:** Graph of HCC TVDT (expressed in days) in observational studies. The median doubling time of primary HCC is 178 days and that of recurrent HCC is 82 days.

liver ranges from 17 to 178 months (105,106). Hemangiomas are uncommon in livers with advanced cirrhosis, however, with a large series showing hemangiomas in only nine of 508 explanted livers (1.7%) (107). Although the low prevalence of these lesions in cirrhosis is not entirely understood, the aforementioned study reported areas of fibrosis surrounding the nine hemangiomas at pathologic examination, suggesting they are obliterated by cirrhotic scarring. With progressive fibrosis, hemangiomas in cirrhotic livers frequently become smaller and are associated with capsular retraction (108). Thus, in the setting of cirrhosis, a growing mass is highly unlikely to be a hemangioma.

*Knowledge gaps.*—The effect of antiviral and antifibrotic therapy on the TVDT of HCC is unknown.

Despite reports on HCC TVDT, there is a lack of data on the TVDT of non-HCC observations in cirrhosis. Further research is required to determine whether specific growth thresholds may permit differentiation of HCCs from benign (eg, cirrhosis associated nodules), premalignant (eg, dysplastic nodules), and other malignant tumors (eg, ICC).

A limitation of growth as a diagnostic criterion is that its diagnostic performance for the diagnosis of HCC has not been assessed prospectively. Doing so would require further validation in a representative sample of untreated observations with imaging features diagnostic of HCC. However, because of the availability of curative and palliative treatment options for HCC, it would be unethical to prospectively assess the diagnostic accuracy of growth thresholds while withholding

treatment. Determination of growth rate by retrospective detection on prior false-negative images (86) introduces substantial selection bias, likely favoring well-differentiated tumors that have less obvious imaging features. Hence, the evidence in favor of tumor growth is likely to remain indirect, based on observational studies. The knowledge gaps listed above regarding observation diameter are also applicable to threshold growth. Cross-modality comparisons between CT and MR imaging may introduce a source of measurement variability in addition to those related to sequence, phase, and imaging plan.

*Summary.*—Although prospectively validated estimates of diagnostic accuracy are lacking, indirect evidence and biologic plausibility indicate that growth is a feature of malignancy and helps to differentiate HCC from benign entities. Growth is not specific for HCC, however, and there is no evidence or plausible basis to suggest that it can differentiate HCC from non-HCC malignancies.

**Recommendation:**

5. Threshold growth should be a major criterion for diagnosis of HCC.

Quality of evidence: Low.

Strength of recommendation in favor of diagnostic criterion: Strong.

### 6. Imaging Features Suggesting Malignancy Other than HCC (LR-M)

*Literature review question.*—In patients at risk for HCC, what imaging features suggest ICC rather than HCC?

*Definition.*—In LI-RADS, LR-M is defined as a probable or definite malignancy, not specific for HCC. A mass with features suggestive of malignancy (diffusion restriction, growth, signal intensity different than background liver-T2 hyperintensity, iron or fat sparing) but lacking specific features of HCC (classic APHE and washout/capsule appearance, intralesional fat or blood products) may be appropriately classified as LR-M. To preserve specificity for diagnosis of HCC, it is important to identify and appropriately classify malignant observations that either demonstrate features of other malignancies (most commonly intrahepatic mass forming cholangiocarcinoma, ICC) or lack imaging features that are sufficiently specific for HCC. LR-M observations may still be HCC, but may also represent other malignancies, such as ICC, hepatocholangiocarcinomas, or metastases.

*Biologic basis and rationale.*—The most common malignancy other than HCC in the setting of chronic liver disease is ICC. Compared with HCCs, ICCs tend to be more cellular and vascular at their periphery while having a more fibrotic and watery stroma centrally. This concentric histologic structure accounts for the characteristic "targetoid" enhancement pattern of these lesions: APHE of the vascularized periphery, creating a rimlike pattern; subsequent wash out appearance of the lesion periphery; and delayed or progressive contrast agent accumulation centrally within the watery stroma. Similarly, a targetoid pattern has been described on diffusion weighted images: The outer cellular zone tends to demonstrate more diffusion restriction than the central more watery core. A targetoid pattern may be present in the hepatobiliary phase with hepatobiliary contrast agents: central mild retention of contrast material, thought to be due to trapping of contrast materialin the fibrotic stroma, in combination with lack of retention in the cholangiocellular periphery.

Hepatocholangiocarcinomas are rare primary "biphenotypic" hepatic malignancies that may show features overlapping HCC and ICC (109). Some authors suggest that the imaging features more closely resemble those of ICC and that prospective differentiation of ICC from a combined tumor can be difficult (109–111).

*Evidence.*—The search query identified 19 studies. After reviewing the abstracts, all these studies were considered relevant and the full text of each was reviewed. All the included studies were retrospective.

Four included studies described the dynamic postcontrast imaging features of ICC on CT and MR images with extracellular and hepatobiliary contrast agents (112–115). While there are varying descriptions of APHE patterns, rimlike APHE is the most commonly reported among the included studies, being present in 50%–84% of reported lesions, depending on the study. As mentioned above, rimlike APHE suggests malignancy other than HCC whereas APHE not limited to a rim favors HCC. At portal venous and delayed phase imaging with extracellular agents, a pattern of delayed or progressive central enhancement emerges was reported in 42%–96% of lesions. A targetoid pattern characterized by rimlike or peripheral APHE and progressive delayed central enhancement may depend on lesion size. Small ICC (< 3 cm) may not display this pattern, and differentiation from HCC can be challenging (116). Washout appearance is less well described and presents an added challenge in deciphering the literature. Few authors made a distinction between peripheral and nonperipheral "washout" patterns. Additionally, with gadoxetate disodium–enhanced MR imaging, distinction between "washout appearance" assessed on the portal venous phase images from hypointensity in the transitional or hepatobiliary phases is not always made clear in the publication (113,114). Despite these potential confounding factors, "washout" is described in a minority (4%–6%) of cases with ICC (113–115). Capsule appearance is even less commonly described for ICC (87), which is not surprising since ICCs do not have true tumor capsules pathologically.

Other ancillary features associated with ICC include hepatic capsular retraction, peripheral biliary duct dilation, central T2 hypointensity, and target appearance on diffusion-weighted images (113–115,117–120).

While there is ample evidence supporting the classic imaging features of ICC, few studies test the ability of these features to help differentiate ICC from HCC, and fewer studies focus on these lesions in patients with defined risk factors or cirrhosis (ie, the LI-RADS population) (87,116,117,119,121–123). The studies that have attempted to determine the discriminatory power of diagnostic imaging for differentiating HCC from ICC have focused on atypical HCC in the comparator group. Despite these

limitations, target appearance on hepatobiliary phase images and presence of rimlike APHE and peripheral "washout" may help differentiate ICC from HCC (113,117).

To date, only a few publications have described the imaging appearance of hepatocholangiocarcinomas. The evolving pathologic definition of this tumor type and the inconsistent use of radiologic terminology to describe it limits the conclusions that can be drawn. A majority of cases report rim APHE with washout appearance in the periphery (86,110,120,124–130). In combination with delayed central enhancement (110,128), these imaging features are similar to ICC described above. Rarely, these tumors may display features of HCC, including diffuse APHE and nonperipheral washout appearance, or have both HCC and ICC features (124,129,130). The preponderance of HCC or ICC imaging features may correspond to lesional pathologic features (124,129). Unlike HCC, these tumors frequently arise in patients without cirrhosis or known risk factors for HCC (110,127,130).

*Knowledge gaps.*—A number of studies have described the appearance of ICC in both cirrhotic and noncirrhotic patients, with or without hepatitis or other risk factors for HCC. However, most of these studies have not explicitly separated the appearance of ICC in patients with from those without chronic liver disease or risk factors for HCC (86,113,117,119,122). It is not known whether ICCs arising in the setting of chronic liver disease and cirrhosis have a similar imaging appearance to those arising in absence of risk factors. Additionally, some prior literature did not clearly separate intrahepatic from periductal infiltrating cholangiocarcinomas.

Given the rarity of non-HCC malignancies and relative absence of predictable risk factors for mass-forming ICC, all of the current evidence is retrospective and comprises single-center experiences. No prospective data are available to better quantify the diagnostic accuracy of the above described imaging features. It is believed that many, if not most, observations categorized as LR-M are probably atypical HCCs due to the higher pretest probability of HCC in at-risk patients, but this is unknown and needs further study.

In regard to hepatocholangiocarcinomas, the optimal management and prognosis are not well known. While resection appears to offer the best survival advantage in most patients, transplantation and hepatic-directed therapies have been suggested as alternative options in patients who cannot undergo resection due to underlying liver disease. The AASLD and the OPTN/UNOS do not currently provide guidance on the diagnosis or transplant eligibility of these patients.

*Summary.*—Emerging evidence suggests that a targetoid imaging appearance at dynamic imaging, diffusion-weighted imaging, and hepatobiliary phase imaging suggests the possibility of ICC or hepatocholangiocarcinoma. The targetoid appearance may be attributable the concentric structure typical of ICC pathologically, with cellular and vascular elements in the periphery and stromal fibrosis in the center.

**Recommendation:**

6. LR-M should be chosen over other LI-RADS categories when an observation has a targetoid imaging appearance—characterized by one or more of the following: rim APHE, delayed central enhancement, target appearance at hepatobiliary phase imaging, target appearance at diffusion-weighted imaging—and no imaging features indicating hepatocellular origin.

Quality of evidence: Moderate.

Strength of recommendation in favor of diagnostic criterion: Strong.

## Conclusion

Unlike other cancers, the definitive diagnosis and staging of HCC is frequently based on imaging without mandatory histopathologic confirmation. The aim of imaging-based diagnostic criteria is to achieve near-100% specificity for the noninvasive diagnosis of HCC.

LI-RADS major imaging criteria currently include APHE, observation diameter, "washout," "capsule," and threshold growth. In this review article, we summarized the evidence, assessed the level of evidence, identified knowledge gaps, and evaluated the strength of recommendations supporting the inclusion of each major criterion for diagnosis of HCC, as well as imaging features indicative of malignancy other than HCC.

**Author affiliations:** Department of Radiology, Université de Montréal, 1058 rue Saint-Denis, Montréal, QC, Canada H2X 3J4 (A.T., K.N.V.); Department of Radiology and Center for Advanced Magnetic Resonance Development, Duke University Medical Center, Durham, NC (M.R.B.); Department of Radiology, Davis Medical Center, University of California, Sacramento, Calif (M.T.C.); Inland Imaging, Spokane, Wash (I.C.); Caritas-Krankenhaus, Medizinische Klinik 2, Bad Mergentheim, Germany (C.F.D.); Department of Radiology, Memorial Sloan-Kettering Cancer Center, New York, NY (R.K.G.D.); Department of Radiology, Mayo Clinic, Rochester, Minn (E.C.E.); Mallinckrodt Institute of Radiology, Washington University School of Medicine, St Louis, Mo (K.J.F.); Department of Radiology, University of Michigan Health System, Ann Arbor, Mich (H.K.H.); Department of Radiology, American University of Beirut, Beirut, Lebanon (H.K.H.); Department of Radiology, MedStar Georgetown University Hospital, Washington, DC (R.C.J.); Department of Radiology, University of Massachusetts Medical School, Worcester, Mass (A.R.K.); Department of Radiology, Liver Imaging Group, University of California San Diego, Calif (A.M., C.B.S.); Department of Radiology, Naval Medical Center San Diego, San Diego, Calif (R.M.M.); Department of Radiology, Thomas Jefferson University, Philadelphia, Pa (D.G.M.); Department of Radiology and Biomedical Imaging, University of California San Francisco, San Francisco, Calif (T.A.M., M.A.O.); Zuckerberg San Francisco General Hospital, San Francisco, Calif (M.A.O.); and Department of Radiology, Hospital of the University of Pennsylvania, Philadelphia, Pa (A.S.).

**Acknowledgment:** The views expressed in this presentation are those of the authors and do not necessarily reflect the official policy or position of the Department of the Navy, Department of Defense, or the United States Government. The author(s) are military service members. This work was prepared as part of official duties. Title 17 U.S.C. 105 provides that Copyright protection under this title is not available for any work of the United States Government.

**Disclosures of Conflicts of Interest: A.T.** disclosed no relevant relationships. **M.R.B.** Activities related to the present article: disclosed no relevant relationships. Activities not related to the present article: grants from Siemens Healthcare, GE Healthcare, NGM Biopharmaceuticals, TaiwanJ Pharma, and Madrigal Pharmaceuticals; consulting fees from RadMD. Other relationships: disclosed no relevant relationships. **M.T.C.** disclosed no relevant relationships. **I.C.** disclosed no relevant relationships. **C.F.D.** disclosed no relevant relationships. **R.K.G.D.** disclosed no relevant relationships. **E.C.E.** disclosed no rele-

vant relationships. **K.J.F.** disclosed no relevant relationships. **H.K.H.** disclosed no relevant relationships. **R.C.J.** disclosed no relevant relationships. **A.R.K.** disclosed no relevant relationships. **A.M.** disclosed no relevant relationships. **R.M.M.** disclosed no relevant relationships. **D.G.M.** disclosed no relevant relationships. **T.A.M.** disclosed no relevant relationships. **M.A.O.** Activities related to the present article: disclosed no relevant relationships. Activities not related to the present article: grant from Gilead Pharmaceuticals, co-investigator limited to reading research scans. Other relationships: disclosed no relevant relationships. **A.S.** disclosed no relevant relationships. **K.N.V.** disclosed no relevant relationships. **C.B.S.** disclosed no relevant relationships.

## References

1. Tang A, Cruite I, Sirlin CB. Toward a standardized system for hepatocellular carcinoma diagnosis using computed tomography and MRI. Expert Rev Gastroenterol Hepatol 2013;7(3):269–279.
2. Santillan CS, Tang A, Cruite I, Shah A, Sirlin CB. Understanding LI-RADS: a primer for practical use. Magn Reson Imaging Clin N Am 2014;22(3):337–352.
3. Tang A, Valasek MA, Sirlin CB. Update on the Liver Imaging Reporting and Data System: what the pathologist needs to know. Adv Anat Pathol 2015;22(5):314–322.
4. Bruix J, Sherman M; American Association for the Study of Liver Diseases. Management of hepatocellular carcinoma: an update. Hepatology 2011;53(3):1020–1022.
5. Park MS, Kim S, Patel J, et al. Hepatocellular carcinoma: detection with diffusion-weighted versus contrast-enhanced magnetic resonance imaging in pretransplant patients. Hepatology 2012;56(1):140–148.
6. Song P, Tobe RG, Inagaki Y, et al. The management of hepatocellular carcinoma around the world: a comparison of guidelines from 2001 to 2011. Liver Int 2012;32(7):1053–1063.
7. Hanna RF, Kased N, Kwan SW, et al. Double-contrast MRI for accurate staging of hepatocellular carcinoma in patients with cirrhosis. AJR Am J Roentgenol 2008;190(1):47–57.
8. Ito K, Mitchell DG, Siegelman ES. Cirrhosis: MR imaging features. Magn Reson Imaging Clin N Am 2002;10(1):75–92, vi.
9. Heimbach J, Kulik LM, Finn R, et al. AASLD guidelines for the treatment of hepatocellular carcinoma. Hepatology 2017 Jan 28.
10. Cruite I, Tang A, Sirlin CB. Imaging-based diagnostic systems for hepatocellular carcinoma. AJR Am J Roentgenol 2013;201(1):41–55.
11. OPTN/UNOS policy 9: Allocation of Livers and Liver-Intestines. https://optn.transplant.hrsa.gov/ContentDocuments/OPTN_Policies.pdf-nameddest=Policy_09. Published 2015. Accessed April 27, 2015.
12. Mitchell DG, Bruix J, Sherman M, Sirlin CB. LI-RADS (Liver Imaging Reporting and Data System): summary, discussion, and consensus of the LI-RADS Management Working Group and future directions. Hepatology 2015;61(3):1056–1065.
13. AASLD Guideline policies, including the AASLD Policy on the Development and Use of Practice Guidelines and the American Gastroenterology Association Policy Statement on Guidelines. https://www.aasld.org/sites/default/files/documents/AASLD_Practice_Guidelines_Development_Policy_12-19-2011.pdf. Published 2009. Accessed April 5, 2015.
14. Guyatt GH, Oxman AD, Vist GE, et al. GRADE: an emerging consensus on rating quality of evidence and strength of recommendations. BMJ 2008;336(7650):924–926.
15. Park YN, Yang CP, Fernandez GJ, Cubukcu O, Thung SN, Theise ND. Neoangiogenesis and sinusoidal "capillarization" in dysplastic nodules of the liver. Am J Surg Pathol 1998;22(6):656–662.
16. Matsui O. Imaging of multistep human hepatocarcinogenesis by CT during intra-arterial contrast injection. Intervirology 2004;47(3-5):271–276.
17. Kim TK, Lee KH, Jang HJ, et al. Analysis of gadobenate dimeglumine-enhanced MR findings for characterizing small (1-2-cm) hepatic nodules in patients at high risk for hepatocellular carcinoma. Radiology 2011;259(3):730–738.
18. Lee KH, O'Malley ME, Haider MA, Hanbidge A. Triple-phase MDCT of hepatocellular carcinoma. AJR Am J Roentgenol 2004;182(3):643–649.
19. Oliver JH 3rd, Baron RL, Federle MP, Rockette HE Jr. Detecting hepatocellular carcinoma: value of unenhanced or arterial phase CT imaging or both used in conjunction with conventional portal venous phase contrast-enhanced CT imaging. AJR Am J Roentgenol 1996;167(1):71–77.
20. Yamashita Y, Mitsuzaki K, Yi T, et al. Small hepatocellular carcinoma in patients with chronic liver damage: prospective comparison of detection with dynamic MR imaging and helical CT of the whole liver. Radiology 1996;200(1):79–84.
21. Sangiovanni A, Manini MA, Iavarone M, et al. The diagnostic and economic impact of contrast imaging techniques in the diagnosis of small hepatocellular carcinoma in cirrhosis. Gut 2010;59(5):638–644.
22. Rimola J, Forner A, Tremosini S, et al. Non-invasive diagnosis of hepatocellular carcinoma ≤ 2 cm in cirrhosis. Diagnostic accuracy assessing fat, capsule and signal intensity at dynamic MRI. J Hepatol 2012;56(6):1317–1323.
23. Burrel M, Llovet JM, Ayuso C, et al. MRI angiography is superior to helical CT for detection of HCC prior to liver transplantation: an explant correlation. Hepatology 2003;38(4):1034–1042.
24. Denecke T, Grieser C, Fröling V, et al. Multislice computed tomography using a triple-phase contrast protocol for preoperative assessment of hepatic tumor load in patients with hepatocellular carcinoma before liver transplantation. Transpl Int 2009;22(4):395–402.
25. Sano K, Ichikawa T, Motosugi U, et al. Imaging study of early hepatocellular carcinoma: usefulness of gadoxetic acid-enhanced MR imaging. Radiology 2011;261(3):834–844.
26. Jang HJ, Kim TK, Khalili K, et al. Characterization of 1- to 2-cm liver nodules detected on hcc surveillance ultrasound according to the criteria of the American Association for the Study of Liver Disease: Is quadriphasic CT necessary? AJR Am J Roentgenol 2013;201(2):314–321.
27. Park MJ, Kim YK, Lee MH, Lee JH. Validation of diagnostic criteria using gadoxetic acid-enhanced and diffusion-weighted MR imaging for small hepatocellular carcinoma (≤ 2.0 cm) in patients with hepatitis-induced liver cirrhosis. Acta Radiol 2013;54(2):127–136.
28. Valls C, Cos M, Figueras J, et al. Pretransplantation diagnosis and staging of hepatocellular carcinoma in patients with cirrhosis: value of dual-phase helical CT. AJR Am J Roentgenol 2004;182(4):1011–1017.
29. Forner A, Vilana R, Ayuso C, et al. Diagnosis of hepatic nodules 20 mm or smaller in cirrhosis: Prospective validation of the noninvasive diagnostic criteria for hepatocellular carcinoma. Hepatology 2008;47(1):97–104.
30. Luca A, Caruso S, Milazzo M, et al. Multidetector-row computed tomography (MDCT) for the diagnosis of hepatocellular carcinoma in cirrhotic candidates for liver transplantation: prevalence of radiological vascular patterns and histological correlation with liver explants. Eur Radiol 2010;20(4):898–907.
31. Sersté T, Barrau V, Ozenne V, et al. Accuracy and disagreement of computed tomography and magnetic resonance imaging for the diagnosis of small hepatocellular carcinoma and dysplastic nodules: role of biopsy. Hepatology 2012;55(3):800–806.

32. van den Bos IC, Hussain SM, Dwarkasing RS, et al. MR imaging of hepatocellular carcinoma: relationship between lesion size and imaging findings, including signal intensity and dynamic enhancement patterns. J Magn Reson Imaging 2007;26(6):1548–1555.

33. Kudo M, Izumi N, Kokudo N, et al. Management of hepatocellular carcinoma in Japan: Consensus-Based Clinical Practice Guidelines proposed by the Japan Society of Hepatology (JSH) 2010 updated version. Dig Dis 2011;29(3):339–364.

34. Omata M, Lesmana LA, Tateishi R, et al. Asian Pacific Association for the Study of the Liver consensus recommendations on hepatocellular carcinoma. Hepatol Int 2010;4(2):439–474.

35. European Association For The Study Of The Liver; European Organisation For Research And Treatment Of Cancer. EASL-EORTC clinical practice guidelines: management of hepatocellular carcinoma. J Hepatol 2012;56(4):908–943.

36. Earls JP, Theise ND, Weinreb JC, et al. Dysplastic nodules and hepatocellular carcinoma: thin-section MR imaging of explanted cirrhotic livers with pathologic correlation. Radiology 1996;201(1):207–214.

37. Korean Liver Cancer Study Group (KLCSG); National Cancer Center, Korea (NCC). 2014 Korean Liver Cancer Study Group-National Cancer Center Korea practice guideline for the management of hepatocellular carcinoma. Korean J Radiol 2015;16(3):465–522.

38. An C, Park MS, Kim D, et al. Added value of subtraction imaging in detecting arterial enhancement in small (<3 cm) hepatic nodules on dynamic contrast-enhanced MRI in patients at high risk of hepatocellular carcinoma. Eur Radiol 2013;23(4):924–930.

39. Shinagawa T, Ohto M, Kimura K, et al. Diagnosis and clinical features of small hepatocellular carcinoma with emphasis on the utility of real-time ultrasonography: a study in 51 patients. Gastroenterology 1984;86(3):495–502.

40. Watanabe A, Yamamoto H, Ito T, Nagashima H. Diagnosis, treatment and prognosis of small hepatocellular carcinoma. Hepatogastroenterology 1986;33(2):52–55.

41. Kitamoto M, Nakanishi T, Kira S, et al. The assessment of proliferating cell nuclear antigen immunohistochemical staining in small hepatocellular carcinoma and its relationship to histologic characteristics and prognosis. Cancer 1993;72(6):1859–1865.

42. Bartolozzi C, Lencioni R, Caramella D, Palla A, Bassi AM, Di Candio G. Small hepatocellular carcinoma: detection with US, CT, MR imaging, DSA, and lipiodol-CT. Acta Radiol 1996;37(1):69–74.

43. Sakabe K, Yamamoto T, Kubo S, et al. Correlation between dynamic computed tomographic and histopathological findings in the diagnosis of small hepatocellular carcinoma. Dig Surg 2004;21(5-6):413–420.

44. Wen YL, Zhou P, Kudo M. Detection of intratumoral vascularity in small hepatocellular carcinoma by coded phase inversion harmonics. Intervirology 2004;47(3-5):169–178.

45. Wang H, Wang XY, Jiang XX, Ye ZX. Comparison of diffusion-weighted with T2-weighted imaging for detection of small hepatocellular carcinoma in cirrhosis: preliminary quantitative study at 3-T. Acad Radiol 2010;17(2):239–243.

46. Kim YK, Kim CS, Han YM, Yu HC, Choi D. Detection of small hepatocellular carcinoma: intraindividual comparison of gadoxetic acid-enhanced MRI at 3.0 and 1.5 T. Invest Radiol 2011;46(6):383–389.

47. Fowler KJ, Karimova EJ, Arauz AR, et al. Validation of organ procurement and transplant network (OPTN)/united network for organ sharing (UNOS) criteria for imaging diagnosis of hepatocellular carcinoma. Transplantation 2013;95(12):1506–1511.

48. Takayama T, Makuuchi M, Hirohashi S, et al. Malignant transformation of adenomatous hyperplasia to hepatocellular carcinoma. Lancet 1990;336(8724):1150–1153.

49. Horigome H, Nomura T, Saso K, Itoh M, Joh T, Ohara H. Limitations of imaging diagnosis for small hepatocellular carcinoma: comparison with histological findings. J Gastroenterol Hepatol 1999;14(6):559–565.

50. Tanaka Y, Sasaki Y, Katayama K, et al. Probability of hepatocellular carcinoma of small hepatocellular nodules undetectable by computed tomography during arterial portography. Hepatology 2000;31(4):890–898.

51. Hamilton AL Sr. Tumours of the liver and intrahepatic bile ducts. In: World Health Organization Classification of Tumours. Lyon, France: IARC, 2000; 159–172.

52. Ohkawa K, Imanaka K, Sakakibara M, et al. Factors related to shift from hepatic borderline lesion to overt HCC diagnosed by CT. Hepatogastroenterology 2014;61(134):1680–1687.

53. Bolondi L, Gaiani S, Celli N, et al. Characterization of small nodules in cirrhosis by assessment of vascularity: the problem of hypovascular hepatocellular carcinoma. Hepatology 2005;42(1):27–34.

54. Yoo HJ, Lee JM, Lee JY, et al. Additional value of SPIO-enhanced MR imaging for the noninvasive imaging diagnosis of hepatocellular carcinoma in cirrhotic liver. Invest Radiol 2009;44(12):800–807.

55. Chen L, Zhang L, Liang M, et al. Magnetic resonance imaging with gadoxetic acid disodium for the detection of hepatocellular carcinoma: a meta-analysis of 18 studies. Acad Radiol 2014;21(12):1603–1613.

56. Khan AS, Hussain HK, Johnson TD, Weadock WJ, Pelletier SJ, Marrero JA. Value of delayed hypointensity and delayed enhancing rim in magnetic resonance imaging diagnosis of small hepatocellular carcinoma in the cirrhotic liver. J Magn Reson Imaging 2010;32(2):360–366.

57. Becker-Weidman DJ, Kalb B, Sharma P, et al. Hepatocellular carcinoma lesion characterization: single-institution clinical performance review of multiphase gadolinium-enhanced MR imaging—comparison to prior same-center results after MR systems improvements. Radiology 2011;261(3):824–833.

58. Liu X, Zou L, Liu F, Zhou Y, Song B. Gadoxetic acid disodium-enhanced magnetic resonance imaging for the detection of hepatocellular carcinoma: a meta-analysis. PLoS One 2013;8(8):e70896.

59. Wu LM, Xu JR, Gu HY, et al. Is liver-specific gadoxetic acid-enhanced magnetic resonance imaging a reliable tool for detection of hepatocellular carcinoma in patients with chronic liver disease? Dig Dis Sci 2013;58(11):3313–3325.

60. Compagnon P, Grandadam S, Lorho R, et al. Liver transplantation for hepatocellular carcinoma without preoperative tumor biopsy. Transplantation 2008;86(8):1068–1076.

61. Golfieri R, Renzulli M, Lucidi V, Corcioni B, Trevisani F, Bolondi L. Contribution of the hepatobiliary phase of Gd-EOB-DTPA-enhanced MRI to dynamic MRI in the detection of hypovascular small (≤ 2 cm) HCC in cirrhosis. Eur Radiol 2011;21(6):1233–1242.

62. Chou R, Cuevas C, Fu R, et al. Imaging techniques for the diagnosis of hepatocellular carcinoma: a systematic review and meta-analysis. Ann Intern Med 2015;162(10):697–711.

63. Haradome H, Grazioli L, Tinti R, et al. Additional value of gadoxetic acid-DTPA-enhanced hepatobiliary phase MR imaging in the diagnosis of early-stage hepatocellular carcinoma: comparison with dynamic triple-phase multidetector CT imaging. J Magn Reson Imaging 2011;34(1):69–78.

64. Barth BK, Donati OF, Fischer MA, et al. Reliability, validity, and reader acceptance

of LI-RADS: an in-depth analysis. Acad Radiol 2016;23(9):1145–1153.

65. Bashir MR, Huang R, Mayes N, et al. Concordance of hypervascular liver nodule characterization between the organ procurement and transplant network and liver imaging reporting and data system classifications. J Magn Reson Imaging 2015;42(2):305–314.

66. Davenport MS, Khalatbari S, Liu PS, et al. Repeatability of diagnostic features and scoring systems for hepatocellular carcinoma by using MR imaging. Radiology 2014;272(1):132–142.

67. Joo I, Lee JM, Lee DH, Ahn SJ, Lee ES, Han JK. Liver imaging reporting and data system v2014 categorization of hepatocellular carcinoma on gadoxetic acid-enhanced MRI: Comparison with multiphasic multidetector computed tomography. J Magn Reson Imaging 2017;5(3):731–740.

68. Sofue K, Sirlin CB, Allen BC, Nelson RC, Berg CL, Bashir MR. How reader perception of capsule affects interpretation of washout in hypervascular liver nodules in patients at risk for hepatocellular carcinoma. J Magn Reson Imaging 2016;43(6):1337–1345.

69. Zhang YD, Zhu FP, Xu X, et al. Classifying CT/MR findings in patients with suspicion of hepatocellular carcinoma: comparison of liver imaging reporting and data system and criteria-free Likert scale reporting models. J Magn Reson Imaging 2016;43(2):373–383.

70. Bultman EM, Brodsky EK, Horng DE, et al. Quantitative hepatic perfusion modeling using DCE-MRI with sequential breathholds. J Magn Reson Imaging 2014;39(4):853–865.

71. Salmani Rahimi M, Korosec FR, Wang K, et al. Combined dynamic contrast-enhanced liver MRI and MRA using interleaved variable density sampling. Magn Reson Med 2015;73(3):973–983.

72. Marrero JA, Hussain HK, Nghiem HV, Umar R, Fontana RJ, Lok AS. Improving the prediction of hepatocellular carcinoma in cirrhotic patients with an arterially-enhancing liver mass. Liver Transpl 2005;11(3):281–289.

73. Cereser L, Furlan A, Bagatto D, et al. Comparison of portal venous and delayed phases of gadolinium-enhanced magnetic resonance imaging study of cirrhotic liver for the detection of contrast washout of hypervascular hepatocellular carcinoma. J Comput Assist Tomogr 2010;34(5):706–711.

74. Liu YI, Shin LK, Jeffrey RB, Kamaya A. Quantitatively defining washout in hepatocellular carcinoma. AJR Am J Roentgenol 2013;200(1):84–89.

75. Nakamura Y, Toyota N, Date S, et al. Clinical significance of the transitional phase at gadoxetate disodium-enhanced hepatic MRI for the diagnosis of hepatocellular carcinoma: preliminary results. J Comput Assist Tomogr 2011;35(6):723–727.

76. Choi SH, Byun JH, Kim SY, et al. Liver Imaging Reporting and Data System v2014 With gadoxetate disodium-enhanced magnetic resonance imaging: validation of LI-RADS category 4 and 5 criteria. Invest Radiol 2016;51(8):483–490.

77. Joo I, Lee JM, Lee DH, Jeon JH, Han JK, Choi BI. Noninvasive diagnosis of hepatocellular carcinoma on gadoxetic acid-enhanced MRI: can hypointensity on the hepatobiliary phase be used as an alternative to washout? Eur Radiol 2015;25(10):2859–2868.

78. Ishigami K, Yoshimitsu K, Nishihara Y, et al. Hepatocellular carcinoma with a pseudocapsule on gadolinium-enhanced MR images: correlation with histopathologic findings. Radiology 2009;250(2):435–443.

79. Okuda K, Musha H, Nakajima Y, et al. Clinicopathologic features of encapsulated hepatocellular carcinoma: a study of 26 cases. Cancer 1977;40(3):1240–1245.

80. Edmondson HA, Steiner PE. Primary carcinoma of the liver: a study of 100 cases among 48,900 necropsies. Cancer 1954;7(3):462–503.

81. Ishizaki M, Ashida K, Higashi T, et al. The formation of capsule and septum in human hepatocellular carcinoma. Virchows Arch 2001;438(6):574–580.

82. Nakayama H, Enzan H, Yamamoto M, Miyazaki E, Yasui W. High molecular weight caldesmon positive stromal cells in the capsule of hepatocellular carcinomas. J Clin Pathol 2004;57(7):776–777.

83. International Consensus Group for Hepatocellular NeoplasiaThe International Consensus Group for Hepatocellular Neoplasia. Pathologic diagnosis of early hepatocellular carcinoma: a report of the international consensus group for hepatocellular neoplasia. Hepatology 2009;49(2):658–664.

84. Ohashi M, Wakai T, Korita PV, Ajioka Y, Shirai Y, Hatakeyama K. Histological evaluation of intracapsular venous invasion for discrimination between portal and hepatic venous invasion in hepatocellular carcinoma. J Gastroenterol Hepatol 2010;25(1):143–149.

85. Ueda K, Matsui O, Kawamori Y, et al. Hypervascular hepatocellular carcinoma: evaluation of hemodynamics with dynamic CT during hepatic arteriography. Radiology 1998;206(1):161–166.

86. Kim SH, Lee CH, Kim BH, et al. Typical and atypical imaging findings of intrahepatic cholangiocarcinoma using gadolinium ethoxybenzyl diethylenetriamine pentaacetic acid-enhanced magnetic resonance imaging. J Comput Assist Tomogr 2012;36(6):704–709.

87. Sheng RF, Zeng MS, Rao SX, Ji Y, Chen LL. MRI of small intrahepatic mass-forming cholangiocarcinoma and atypical small hepatocellular carcinoma (≤3 cm) with cirrhosis and chronic viral hepatitis: a comparative study. Clin Imaging 2014;38(3):265–272.

88. Xu J, Igarashi S, Sasaki M, et al. Intrahepatic cholangiocarcinomas in cirrhosis are hypervascular in comparison with those in normal livers. Liver Int 2012;32(7):1156–1164.

89. American College of Radiology. Liver Imaging Reporting and Data System version 2014. https://www.acr.org/Quality-Safety/Resources/LIRADS/LIRADS-v2014.

90. Wald C, Russo MW, Heimbach JK, Hussain HK, Pomfret EA, Bruix J. New OPTN/UNOS policy for liver transplant allocation: standardization of liver imaging, diagnosis, classification, and reporting of hepatocellular carcinoma. Radiology 2013;266(2):376–382.

91. Bolondi L, Benzi G, Santi V, et al. Relationship between alpha-fetoprotein serum levels, tumour volume and growth rate of hepatocellular carcinoma in a western population. Ital J Gastroenterol 1990;22(4):190–194.

92. Kudo M, Tochio H. Intranodular blood supply correlates well with biological malignancy grade determined by tumor growth rate in pathologically proven hepatocellular carcinoma. Oncology 2008;75(Suppl 1):55–64.

93. Shingaki N, Tamai H, Mori Y, et al. Serological and histological indices of hepatocellular carcinoma and tumor volume doubling time. Mol Clin Oncol 2013;1(6):977–981.

94. Choi D, Mitchell DG, Verma SK, et al. Hepatocellular carcinoma with indeterminate or false-negative findings at initial MR imaging: effect on eligibility for curative treatment initial observations. Radiology 2007;244(3):776–783.

95. Toyoda H, Kumada T, Honda T, et al. Analysis of hepatocellular carcinoma tumor growth detected in sustained responders to interferon in patients with chronic hepatitis C. J Gastroenterol Hepatol 2001;16(10):1131–1137.

96. Tezuka M, Hayashi K, Kubota K, et al. Growth rate of locally recurrent hepatocellular carcinoma after transcatheter arterial chemoembolization: comparing the growth rate of locally recurrent tumor with that of primary hepatocellular carcinoma. Dig Dis Sci 2007;52(3):783–788.

97. Saito Y, Matsuzaki Y, Doi M, et al. Multiple regression analysis for assessing the growth of small hepatocellular carcinoma: the MIB-1 labeling index is the most effective parameter. J Gastroenterol 1998;33(2):229–235.

98. Nakajima T, Moriguchi M, Mitsumoto Y, et al. Simple tumor profile chart based on cell kinetic parameters and histologic grade is useful for estimating the natural growth rate of hepatocellular carcinoma. Hum Pathol 2002;33(1):92–99.

99. Yu JS, Cho ES, Kim KH, Chung WS, Park MS, Kim KW. Newly developed hepatocellular carcinoma (HCC) in chronic liver disease: MR imaging findings before the diagnosis of HCC. J Comput Assist Tomogr 2006;30(5):765–771.

100. Furlan A, Marin D, Agnello F, et al. Hepatocellular carcinoma presenting at contrast-enhanced multi-detector-row computed tomography or gadolinium-enhanced magnetic resonance imaging as a small (≤2 cm), indeterminate nodule: growth rate and optimal interval time for imaging follow-up. J Comput Assist Tomogr 2012;36(1):20–25.

101. Hyodo T, Murakami T, Imai Y, et al. Hypovascular nodules in patients with chronic liver disease: risk factors for development of hypervascular hepatocellular carcinoma. Radiology 2013;266(2):480–490.

102. Jang KM, Kim SH, Kim YK, Choi D. Imaging features of subcentimeter hypointense nodules on gadoxetic acid-enhanced hepatobiliary phase MR imaging that progress to hypervascular hepatocellular carcinoma in patients with chronic liver disease. Acta Radiol 2015;56(5):526–535.

103. Park Y, Choi D, Lim HK, et al. Growth rate of new hepatocellular carcinoma after percutaneous radiofrequency ablation: evaluation with multiphase CT. AJR Am J Roentgenol 2008;191(1):215–220.

104. De Rose AM, Cucchetti A, Clemente G, et al. Prognostic significance of tumor doubling time in mass-forming type cholangiocarcinoma. J Gastrointest Surg 2013;17(4):739–747.

105. Hasan HY, Hinshaw JL, Borman EJ, Gegios A, Leverson G, Winslow ER. Assessing normal growth of hepatic hemangiomas during long-term follow-up. JAMA Surg 2014;149(12):1266–1271.

106. Yeh WC, Yang PM, Huang GT, Sheu JC, Chen DS. Long-term follow-up of hepatic hemangiomas by ultrasonography: with emphasis on the growth rate of the tumor. Hepatogastroenterology 2007;54(74):475–479.

107. Dodd GD 3rd, Baron RL, Oliver JH 3rd, Federle MP. Spectrum of imaging findings of the liver in end-stage cirrhosis: Part II, focal abnormalities. AJR Am J Roentgenol 1999;173(5):1185–1192.

108. Brancatelli G, Federle MP, Blachar A, Grazioli L. Hemangioma in the cirrhotic liver: diagnosis and natural history. Radiology 2001;219(1):69–74.

109. Potretzke TA, Tan BR, Doyle MB, Brunt EM, Heiken JP, Fowler KJ. Imaging features of biphenotypic primary liver carcinoma (hepatocholangiocarcinoma) and the potential to mimic hepatocellular carcinoma: LI-RADS analysis of CT and MRI features in 61 cases. AJR Am J Roentgenol 2016;207(1):25–31.

110. Fowler KJ, Sheybani A, Parker RA 3rd, et al. Combined hepatocellular and cholangiocarcinoma (biphenotypic) tumors: imaging features and diagnostic accuracy of contrast-enhanced CT and MRI. AJR Am J Roentgenol 2013;201(2):332–339.

111. Shetty AS, Fowler KJ, Brunt EM, Agarwal S, Narra VR, Menias CO. Combined hepatocellular-cholangiocarcinoma: what the radiologist needs to know about biphenotypic liver carcinoma. Abdom Imaging 2014;39(2):310–322.

112. Iavarone M, Piscaglia F, Vavassori S, et al. Contrast enhanced CT-scan to diagnose intrahepatic cholangiocarcinoma in patients with cirrhosis. J Hepatol 2013;58(6):1188–1193.

113. Kang Y, Lee JM, Kim SH, Han JK, Choi BI. Intrahepatic mass-forming cholangiocarcinoma: enhancement patterns on gadoxetic acid-enhanced MR images. Radiology 2012;264(3):751–760.

114. Péporté AR, Sommer WH, Nikolaou K, Reiser MF, Zech CJ. Imaging features of intrahepatic cholangiocarcinoma in Gd-EOB-DTPA-enhanced MRI. Eur J Radiol 2013;82(3):e101–e106.

115. Rimola J, Forner A, Reig M, et al. Cholangiocarcinoma in cirrhosis: absence of contrast washout in delayed phases by magnetic resonance imaging avoids misdiagnosis of hepatocellular carcinoma. Hepatology 2009;50(3):791–798.

116. Kim SJ, Lee JM, Han JK, Kim KH, Lee JY, Choi BI. Peripheral mass-forming cholangiocarcinoma in cirrhotic liver. AJR Am J Roentgenol 2007;189(6):1428–1434.

117. Chong YS, Kim YK, Lee MW, et al. Differentiating mass-forming intrahepatic cholangiocarcinoma from atypical hepatocellular carcinoma using gadoxetic acid-enhanced MRI. Clin Radiol 2012;67(8):766–773.

118. Hwang J, Kim YK, Park MJ, et al. Differentiating combined hepatocellular and cholangiocarcinoma from mass-forming intrahepatic cholangiocarcinoma using gadoxetic acid-enhanced MRI. J Magn Reson Imaging 2012;36(4):881–889.

119. Park MJ, Kim YK, Park HJ, Hwang J, Lee WJ. Scirrhous hepatocellular carcinoma on gadoxetic acid-enhanced magnetic resonance imaging and diffusion-weighted imaging: emphasis on the differentiation of intrahepatic cholangiocarcinoma. J Comput Assist Tomogr 2013;37(6):872–881.

120. Willekens I, Hoorens A, Geers C, Op de Beeck B, Vandenbroucke F, de Mey J. Combined hepatocellular and cholangiocellular carcinoma presenting with radiological characteristics of focal nodular hyperplasia. World J Gastroenterol 2009;15(31):3940–3943.

121. Kim YK, Han YM, Kim CS. Comparison of diffuse hepatocellular carcinoma and intrahepatic cholangiocarcinoma using sequentially acquired gadolinium-enhanced and Resovist-enhanced MRI. Eur J Radiol 2009;70(1):94–100.

122. Loyer EM, Chin H, DuBrow RA, David CL, Eftekhari F, Charnsangavej C. Hepatocellular carcinoma and intrahepatic peripheral cholangiocarcinoma: enhancement patterns with quadruple phase helical CT--a comparative study. Radiology 1999;212(3):866–875.

123. Sapisochin G, Fidelman N, Roberts JP, Yao FY. Mixed hepatocellular cholangiocarcinoma and intrahepatic cholangiocarcinoma in patients undergoing transplantation for hepatocellular carcinoma. Liver Transpl 2011;17(8):934–942.

124. Aoki K, Takayasu K, Kawano T, et al. Combined hepatocellular carcinoma and cholangiocarcinoma: clinical features and computed tomographic findings. Hepatology 1993;18(5):1090–1095.

125. de Campos RO, Semelka RC, Azevedo RM, et al. Combined hepatocellular carcinoma-cholangiocarcinoma: report of MR appearance in eleven patients. J Magn Reson Imaging 2012;36(5):1139–1147.

126. Ebied O, Federle MP, Blachar A, et al. Hepatocellular-cholangiocarcinoma: helical computed tomography findings in 30 patients. J Comput Assist Tomogr 2003;27(2):117–124.

127. Jarnagin WR, Weber S, Tickoo SK, et al. Combined hepatocellular and chol-

angiocarcinoma: demographic, clinical, and prognostic factors. Cancer 2002;94(7):2040–2046.

128. Nishie A, Yoshimitsu K, Asayama Y, et al. Detection of combined hepatocellular and cholangiocarcinomas on enhanced CT: comparison with histologic findings. AJR Am J Roentgenol 2005;184(4):1157–1162.

129. Sanada Y, Shiozaki S, Aoki H, Takakura N, Yoshida K, Yamaguchi Y. A clinical study of 11 cases of combined hepatocellular-cholangiocarcinoma Assessment of enhancement patterns on dynamics computed tomography before resection. Hepatol Res 2005;32(3):185–195.

130. Wells ML, Venkatesh SK, Chandan VS, et al. Biphenotypic hepatic tumors: imaging findings and review of literature. Abdom Imaging 2015;40(7):2293–2305.

131. Laghi A, Iannaccone R, Rossi P, et al. Hepatocellular carcinoma: detection with triple-phase multi-detector row helical CT in patients with chronic hepatitis. Radiology 2003;226(2):543–549.

132. Pitton MB, Kloeckner R, Herber S, Otto G, Kreitner KF, Dueber C. MRI versus 64-row MDCT for diagnosis of hepatocellular carcinoma. World J Gastroenterol 2009;15(48):6044–6051.

133. Lopez Hänninen E, Vogl TJ, Bechstein WO, et al. Biphasic spiral computed tomography for detection of hepatocellular carcinoma before resection or orthotopic liver transplantation. Invest Radiol 1998;33(4):216–221.